

**LABORATORY STUDY OF MECHANICAL AND  
SWELLING BEHAVIOR OF COMPACTED  
BENTONITE-AGGREGATE MIXTURES**



**A Thesis Submitted in Partial Fulfillment of the Requirements for the  
Degree of Master of Engineering in Civil, Transportation and  
Geo-Resources Engineering  
Suranaree University of Technology  
Academic Year 2018**

การศึกษาในห้องปฏิบัติการของพฤติกรรมเชิงกลศาสตร์และการบวมตัวของ  
ส่วนผสมของเบนทอไนต์และวัสดุมวลรวมที่ถูกลบอัด



นางสาวลักขิกา สิทธิมงคล

วิทยานิพนธ์นี้เป็นส่วนหนึ่งของการศึกษาตามหลักสูตรปริญญาวิศวกรรมศาสตรมหาบัณฑิต  
สาขาวิชาวิศวกรรมโยธา ขนส่ง และทรัพยากรธรณี  
มหาวิทยาลัยเทคโนโลยีสุรนารี  
ปีการศึกษา 2561

**LABORATORY STUDY OF MECHANICAL AND SWELLING  
BEHAVIOR OF COMPACTED BENTONITE-  
AGGREGATE MIXTURES**

Suranaree University of Technology has approved this thesis submitted in partial fulfillment of the requirements for a Master's Degree.

Thesis Examining Committee



(Asst. Prof. Dr. Akkhapun Wannakomol)

Chairperson



(Prof. Dr. Kittitip Fuenkajorn)

Member (Thesis Advisor)



(Assoc. Prof. Dr. Pornkasem Jongpradist)

Member



(Prof. Dr. Santi Maensiri)

Vice Rector for Academic Affairs  
and Internationalization



(Assoc. Prof. Ft. Lt. Dr. Kontorn Chamniprasart)

Dean of Institute of Engineering

ลักขณา สิทธิมงคล : การศึกษาในห้องปฏิบัติการของพฤติกรรมเชิงกลศาสตร์และการบวมตัวของส่วนผสมของเบนทอไนต์และวัสดุมวลรวมที่ถูกดอัด (LABORATORY STUDY OF MECHANICAL AND SWELLING BEHAVIOR OF COMPACTED BENTONITE-AGGREGATE MIXTURES) อาจารย์ที่ปรึกษา : ศาสตราจารย์ ดร.กิตติเทพ เฟื่องขจร, 68 หน้า.

การทดสอบการบดอัด การเหือนโดยตรงและแรงกดได้ถูกดำเนินการเพื่อหาคุณสมบัติเชิงกลศาสตร์ของส่วนผสมเบนทอไนต์และวัสดุมวลรวมที่บดอัดรวมกับสารละลายแมกนีเซียมคลอไรด์อิ่มตัวสำหรับใช้เป็นวัสดุถมกลับในช่องเหมืองเกลือและเหมืองโปแตช วัสดุมวลรวมประกอบด้วย ดินตะกอนประปา ทราย เกลือหินบด และกรวดที่มีช่องขนาดเม็ดจาก 0.425 ถึง 6 มิลลิเมตร อัตราส่วนผสมของเบนทอไนต์ต่อวัสดุมวลรวมอยู่ระหว่าง 30:70 ถึง 100:0 โดยน้ำหนัก ผลการศึกษาระบุว่าการลดลงของสัดส่วนน้ำหนักเบนทอไนต์สามารถเพิ่มความหนาแน่นแห้งและลดปริมาณน้ำแมกนีเซียมคลอไรด์ที่เหมาะสมได้ ค่าความเค้นยึดติดและมุมเสียดทานมีค่าสูงตามปริมาณการเพิ่มขึ้นของปริมาณและความเหลี่ยมของวัสดุมวลรวม ค่ากำลังกดและโมดูลัสความยืดหยุ่นของส่วนผสมที่มีวัสดุเม็ดละเอียดจะสูงกว่าส่วนผสมที่มีวัสดุเม็ดหยาบและมีค่าเพิ่มขึ้นตามสัดส่วนน้ำหนักของเบนทอไนต์ ด้วยปริมาณเบนทอไนต์ที่มากกว่าทำให้ส่วนผสมภายใต้แรงกดมีการขยายตัวได้มากขึ้นและด้วยเหตุนี้ทำให้อัตราส่วนบวมของสูงขึ้นด้วย ความสามารถในการบวมตัวจะเพิ่มขึ้นเมื่อปริมาณเบนทอไนต์และขนาดเม็ดของวัสดุมวลรวมสูงขึ้น ผลที่ได้สามารถนำมากำหนดพารามิเตอร์การติดตั้งในช่วงแรกและเกณฑ์การคัดสรรวัสดุถมกลับที่ใช้ในช่องเหมืองเกลือและเหมืองโปแตช

สาขาวิชา เทคโนโลยีธรณี

ปีการศึกษา 2561

ลายมือชื่อนักศึกษา ลักขณา สิทธิมงคล

ลายมือชื่ออาจารย์ที่ปรึกษา ก. เฟื่องขจร

LAKSIKAR SITTHIMONGKOL : LABORATORY STUDY OF  
MECHANICAL AND SWELLING BEHAVIOR OF COMPACTED  
BENTONITE-AGGREGATE MIXTURES. THESIS ADVISOR :  
PROF. KITTITEP FUENKAJORN, Ph.D., P.E., 68 PP.

SLUDGE/SAND/CRUSHED SALT/GRAVEL/MAGNESIUM BRINE

Compaction, direct shear, compression tests have been performed to determine mechanical properties of compacted bentonite-aggregate mixtures with saturated magnesium chloride brine for use as backfill in salt and potash mine openings. The aggregates include sludge, sand, crushed salt and gravels. Their grain sizes range from 0.425 to 6 mm. The mixing ratios of the bentonite-to-aggregate are from 30:70 to 100:0 by weight. The results indicate the decrease of the bentonite weight ratio can increase the dry density and decrease the optimum brine content. The cohesions and friction angles increase with increasing aggregate contents and angularity. The compressive strengths and elastic moduli of the mixtures containing finer particles are higher than those with coarser ones. They also increase with the bentonite weight ratio. Higher bentonite contents allow larger dilation of the mixtures under loading, and hence reflecting as higher Poisson's ratio. The swelling capacity increase with increasing bentonite contents and particles size of the aggregates. The findings can be used as initial installation parameters and material selection of backfills employed in salt and potash mine openings.

School of Geotechnolgy

Academic Year 2018

Student's Signature ลักขิณ สิทธิมงคล

Advisor's Signature ค. ฟูเณจอร์น

## ACKNOWLEDGMENTS

I wish to acknowledge the funding supported by Suranaree University of Technology (SUT). I would like to express my sincere thanks to Prof. Dr. Kittitep Fuenkajorn for his valuable guidance and efficient supervision. I appreciate his strong support, encouragement, suggestions and comments during the research period. My heartiness thanks to Assoc. Prof. Dr. Pornkasem Jongpradist and Assist. Dr. Akkhapun Wannakomol, for their constructive advice, valuable suggestions and comments on my research works as thesis committee members. Grateful thanks are given to all staffs of Geomechanics Research Unit, Institute of Engineering who supported my work.

Finally, I would like to thank beloved parents for their love, support and encouragement.

Laksikar Sitthimongkol

มหาวิทยาลัยเทคโนโลยีสุรนารี

# TABLE OF CONTENTS

	<b>Page</b>
ABSTRACT (THAI).....	I
ABSTRACT (ENGLISH).....	II
ACKNOWLEDGEMENTS.....	III
TABLE OF CONTENTS.....	IV
LIST OF TABLES.....	VIII
LIST OF FIGURES.....	IX
SYMBOL AND ABBREVIATIONS.....	XIII
<b>CHAPTER</b>	
<b>I INTRODUCTION.....</b>	<b>1</b>
1.1 Background and Rationale.....	1
1.2 Research Objective.....	2
1.3 Scope and Limitations.....	2
1.4 Research Methodology.....	3
1.4.1 Literature reviews.....	3
1.4.2 Sample collection and preparation.....	4
1.4.3 Compaction test.....	5
1.4.4 Direct Shear test.....	5
1.4.5 Uniaxial compressive strength test.....	5
1.4.6 Swelling tests.....	6

## TABLE OF CONTENTS (Continued)

	Page
1.4.7 Scanning electron microscope analysis.....	7
1.4.8 Discussions and conclusions.....	7
1.4.9 Thesis writing.....	7
1.5 Thesis Contents.....	7
<b>II LITERATURE REVIEW</b> .....	<b>8</b>
2.1 Compaction Test of Backfill Materials in Salt and Potash Openings.....	8
2.2 Direct Shear Test.....	9
2.3 Swelling Test.....	16
2.4 Effect on Hydraulic Conductivity.....	20
2.5 Consolidation Test of Backfill Materials.....	21
<b>III TESTING MATERIALS</b> .....	<b>25</b>
3.1 Introduction.....	25
3.2 Test Materials.....	25
3.2.1 Sieve analysis.....	25
3.2.2 Unified soil classification system.....	27
3.3.3 Sphericity and roughness of aggregates.....	29
3.3 Saturated MgCl <sub>2</sub> Brine.....	30
3.4 Bentonite and Aggregate Mixtures.....	30

## TABLE OF CONTENTS (Continued)

	<b>Page</b>
<b>IV    LABORATORY TESTING</b> .....	33
4.1    Introduction.....	33
4.2    Test Apparatus.....	33
4.3    Compaction Test.....	35
4.3.1    Test method.....	35
4.3.2    Compaction test results.....	36
4.4    Direct Shear Test.....	40
4.3.1    Test method.....	40
4.3.2    Direct shear tests results.....	41
4.5    Uniaxial Compression Test.....	50
4.3.1    Test method.....	50
4.3.2    Uniaxial compression test results.....	50
<b>V     SWELLING TESTS</b> .....	54
5.1    Introduction.....	54
5.2    Swelling Tests under Different Bentonite Weight Ratios.....	55
5.3    Swelling Tests under Different Aggregate Types.....	56
5.4    Swelling Tests under Different Vertical Stresses.....	58
<b>VI    SCANNING ELECTRON MICROSCOPE ANALYSIS</b> .....	61
6.1    Introduction.....	61
6.2    Test Apparatus.....	61

**TABLE OF CONTENTS (Continued)**

	<b>Page</b>
6.3 Test Method.....	62
6.4 Test Results.....	63
<b>VII DISCUSSION AND CONCLUSION.....</b>	<b>65</b>
7.1 Discussion.....	65
7.2 Conclusion.....	67
7.3 Recommendations for Future Studies.....	68
REFERENCES.....	69
BIOGRAPHY.....	77

## LIST OF TABLES

Table	Page
2.1 Comparison of the properties of crushed-salt and salt/bentonite backfill (Butcher, 1991).....	22
3.1 Chemical compositions of the tested bentonite and sludge.....	26
3.2 Classification of bentonite and sludge.....	28
3.3 Classification of sand, fine and coarse gravel.....	28
3.4 Particle shape classification of aggregates based on Powers (1982).....	31
4.1 Compaction test results.....	39
4.2 Direct shear test results.....	49
4.3 Uniaxial compressive test results.....	53
6.1 SEM images of compacted bentonites with $MgCl_2$ and NaCl brines.....	64

## LIST OF FIGURES

Figure	Page
1.1 Research methodology.....	4
2.1 Effect of cation valance on the maximum dry density and optimum water content (Shariatmadari et al., 2011).....	9
2.2 Three-ring mold (Sonsakul and Fuenkajorn, 2013).....	10
2.3 SEM on are dried samples at magnification factors of 75x; a) sand 100%, b) bentonite 5% and c) bentonite 50% (Proia et al., 2016).....	11
2.4 Illustration of particle shape parameters (Yanrong, L., 2013).....	13
2.5 Maximum dry density and optimum water content of bentonite obtained from three-ring mold and ASTM standard mold (Sonsakul et al., 2013).....	14
2.6 Shear stress versus shear displacement response of different sands (Vangla and Latha, 2015).....	15
2.7 Swelling pressure and vertical pressure relation from constant stress tests (Mašín and Khalili, 2015).....	17
2.8 Conceptual diagrams of constant-volume swelling process and microstructure of compacted GMZ01 bentonite (Villar, 2002; Suzuki et al., 2005).....	19
2.9 Swelling test with various NaCl solutions (0, 0.1, 0.5, 1.0 mol/L) under vertical stress of 0.06 MPa (Chen et al., 2016).....	19

## LIST OF FIGURES (Continued)

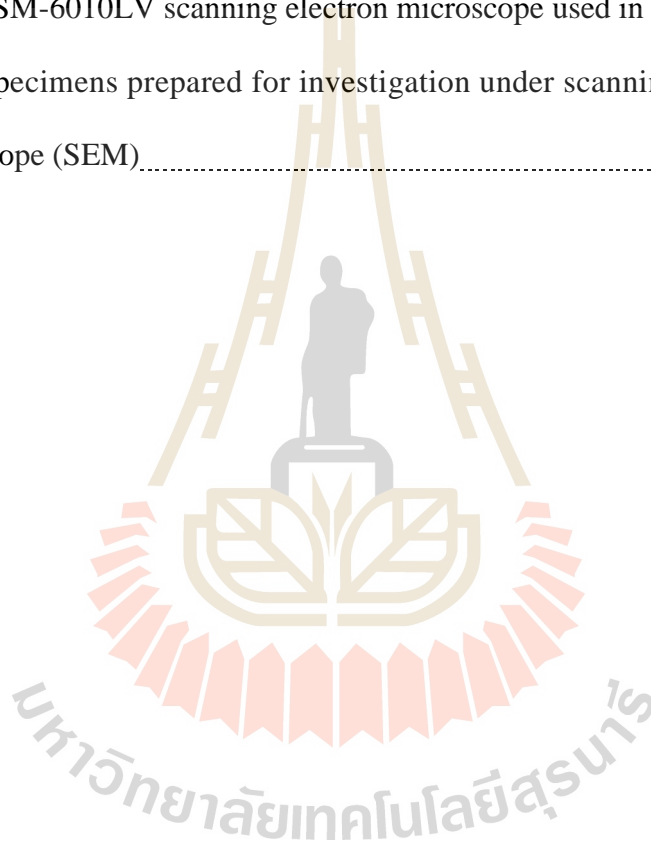
Figure	Page
2.10 Consolidation curve of GMZ07 bentonite by distilled water and 0.5 mol/L NaCl solution (Zhang et al., 2016).....	23
2.11 Consolidation crushed salt with NaCl solution (a) (Khamrat et al., 2017) and with MgCl <sub>2</sub> solution (b) (Suwannabut et al., 2018).....	24
3.1 Particle size distributions of tested materials.....	27
3.2 Size and shape of tested materials.....	30
3.3 Estimation of roundness and sphericity of sedimentary particles (Powers, 1982).....	31
4.1 Three-ring compaction mold (Sonsakul and Fuenkajorn, 2013).....	34
4.2 Direct shear tests frame for three-ring mold (Sonsakul and Fuenkajorn, 2013).....	34
4.3 Maximum dry densities as a function of MgCl <sub>2</sub> brine contents. B = bentonite, SL = sludge, SA = sand, CS = crushed salt, FG = fine gravel and CG = coarse gravel.....	37
4.4 Maximum dry densities (a) and optimum MgCl <sub>2</sub> brine contents (b) as a function of bentonite-to-aggregate weight ratio.....	38
4.5 Shear stress (a) and normal displacement (b) as a function of shear Displacement for bentonite-sludge mixtures.....	42
4.6 Shear stress (a) and normal displacement (b) as a function of shear displacement for bentonite-sand mixtures.....	43

## LIST OF FIGURES (Continued)

Figure	Page
4.7 Shear stress (a) and normal displacement (b) as a function of shear displacement for bentonite-crushed salt mixtures.....	44
4.8 Shear stress (a) and normal displacement (b) as a function of shear displacement for bentonite-fine gravel mixtures.....	45
4.9 Shear stress (a) and normal displacement (b) as a function of shear displacement for bentonite-coarse gravel mixtures.....	46
4.10 Shear strengths as a function normal stress.....	47
4.11 Cohesions (a) and friction angles (b) as a function of bentonite-to-aggregates weight ratio.....	48
4.12 Stress-strain curves of uniaxial compression test.....	51
4.13 Compressive strengths (a), Elastic moduli (b) and Poisson's ratio (c) as a function of bentonite-to-aggregates weight ratio.....	52
5.1 Swelling test in three-ring compaction mold.....	55
5.2 Swelling capacity by various bentonite weight ratios for mixtures with MgCl <sub>2</sub> (a) and NaCl (b) brines.....	57
5.3 Swelling capacity of different aggregate mixtures under MgCl <sub>2</sub> (a) and NaCl (b) brines.....	59

**LIST OF FIGURES (Continued)**

<b>Figure</b>	<b>Page</b>
5.4 Swelling capacity of pure bentonite as a function of vertical stresses, comparing between NaCl and MgCl <sub>2</sub> brine submersions.....	60
6.1 JEOL JSM-6010LV scanning electron microscope used in this studied.....	62
6.2 Some specimens prepared for investigation under scanning electron microscope (SEM).....	63



## SYMBOL AND ABBREVIATIONS

$\varepsilon$	=	Strain
$\nu$	=	Poisson's ratio
$\phi$	=	Angle of friction
$\rho_{\text{Brine}}$	=	Density of saturated magnesium chloride brine
$\rho_{\text{dry}}$	=	Dry density of compacted specimen
$\rho_{\text{H}_2\text{O}}$	=	Density of distilled water
$\rho_{\text{wet}}$	=	Wet density of compacted specimen
$\sigma_c$	=	Compressive strengths
$\sigma_{\text{cons}}$	=	Consolidation stress
$\sigma_n$	=	Normal stress
$\tau$	=	Shear stress
$\text{CaCl}_2$	=	Calcium chloride
$C_c$	=	Coefficient of curvature
CG	=	Coarse gravel
CS	=	Crushed salt
$C_u$	=	Uniformity coefficient
D	=	Swelling ratio
$D_{10}$	=	Particle size at 10% finer
$D_{30}$	=	Particle size at 30% finer

## SYMBOL AND ABBREVIATIONS (Continued)

$D_{60}$	=	Particle size at 60% finer
$d_n$	=	Dilations
$d_s$	=	Shearing displacement
E	=	Elastic moduli
F	=	Shear force
FG	=	Fine gravel
FS	=	Fine sand
GIM	=	Grounding improvement material
H	=	Initial height
$\Delta H$	=	Change of the height
J	=	Compaction energy per unit volume
L	=	Height of drop of hammer
$MgCl_2$	=	Magnesium chloride
MS	=	Medium sand
n	=	Number of blows per layer
NaCl	=	Sodium chloride
P	=	Normal load
SA	=	Sand
SB	=	Solubility of magnesium chloride brine in water
SEM	=	Scanning electron microscope
SL	=	Sludge

**SYMBOL AND ABBREVIATIONS (Continued)**

$t$	=	Number of layers
$V$	=	Volume of mold
$W$	=	Weight of hammer
$W_1$	=	Weight of wet soil and container
$W_2$	=	Weight dry soil and container
$W_b$	=	Magnesium chloride brine content
$W_{can}$	=	Weight of container
$W_i$	=	Initial water content of specimen
XRF	=	X-Ray fluorescence

# CHAPTER I

## INTRODUCTION

### 1.1 Background and Rationale

Thailand mining regulations require that the abandoned salt and potash mine openings be sealed, primarily to reduce the long-term surface subsidence and to minimize waste products obtained from ore processing plants. In addition the sealing materials should be chemically compatible with the surrounding rock (Fuenkajorn and Daemen, 1996). Bentonite has long been extensively used as sealing material due to its low permeability, desirable swelling, self-healing and longevity in nature (Ouyang and Daemen, 1992). A mixture of bentonite and ballast material is also considered as sealant for borehole because it decreases shrinkage potential, increases the bearing capacity of the sealant and minimize creep or settlement (Dixon et al., 1985). Compacted bentonite-based materials have been proposed as possible sealing and sealing materials in geological repositories for the high-level radioactive waste disposal in several countries (Wang, 2014). Borgesson et al. (2003) recommend that the compacted bentonite-crushed salt weight ratio of 30:70 should be used as backfilling in the underground openings. Theerapun et al. (2017) suggest that the halite and carnallite brines should be avoided for backfilling or storing in the potash mine openings. The magnesium brine is suitable for mixing with backfilling material and storing in potash mine openings. For the openings in pure rock salt, sodium, magnesium and carnallite solutions can be used as a mixing component for the backfill material or storage in the mine opening.

This is because the salt is insensitive to these solutions as long as they are under saturated condition.

## 1.2 Research Objective

The objective of this study is to determine the mechanical performance of the compacted bentonite-mixed with aggregates and saturated magnesium brine. The effort includes compaction, direct shear, uniaxial compressive strength and swelling tests on the mixtures. The findings can be used as initial installation parameters for the abandoned salt and potash mine openings.

## 1.3 Scope and Limitations

The scope and limitations of the research include as follows.

- 1) Construction grade bentonite obtained from Thai Nippon Chemical Industry Co., LTD, Thailand.
- 2) The aggregates include:
  - Crushed salt obtained from the Middle members of the Maha Sarakham formation, northeast of Thailand. The grain sizes are ranging from 4 to 6 mm.
  - Sand and gravels obtained from Khok Kruat District, Nakhon Ratchasima Province. They have particle sizes ranging from 1-2, 4-6 and 6.35-9.53 mm, respectively.
  - Sludge (<0.074 mm) obtained from dewatering plant of Bang Khen Water Treatment Plant located in Bangkok Metropolis.
- 3) Saturated brine is prepared from magnesium chloride powder ( $MgCl_2$ ).

- 4) Three-ring compaction and direct shear testing device (Sonsakul and Fuenkajorn, 2013) is used in the compaction and direct shear tests.
- 5) The applied normal stress in the direct shear testing is varied from 0.2, 0.4, 0.6 to 0.8 MPa.
- 6) Uniaxial compression test is carried out on cylindrical specimens with 101.6 mm in diameter and 150 mm in length.
- 7) Swelling test is performed under saturated magnesium and sodium brine. Swelling tests are under different bentonite weight ratios, different aggregate types, and vertical stress tests.
- 8) The pure bentonite mixtures are scanned before and after the swelling test by Scanning Electron Microscope (SEM).
- 9) All testing procedures follow the relevant ASTM standard practice, as much as, practical.
- 10) The research findings are published in conference paper or journal.

## **1.4 Research Methodology**

The research methodology shown in Figure 1.1 comprises 9 steps; including literature review, sample preparation, compaction test, direct shear test, uniaxial compression test, swelling test, scanning electron microscope, discussions and conclusions and thesis writing.

### **1.4.1 Literature Reviews**

Literature reviews are carried out to study the experimental researches on the consolidation test, compaction test and swelling test. The sources of information are

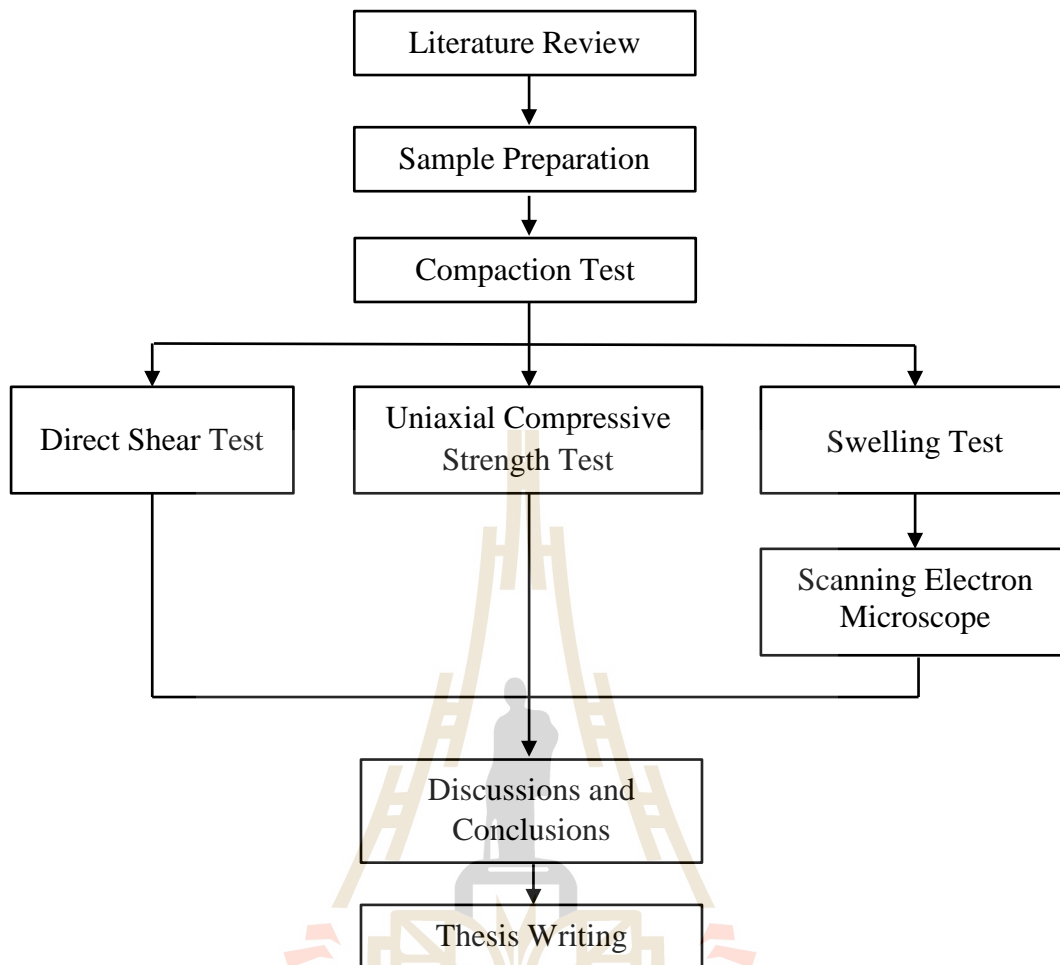


**Figure 1.1** Research methodology.

from textbooks, journals, technical reports and conference papers. A summary of the literature review will be given in the thesis.

#### **1.4.2 Sample collection and Preparation**

Bentonite has been obtained from Thai Nippon Chemical Industry Co., LTD, Thailand. The aggregates are used in this study include sludge (SL), sand (SA), crushed salt (CS), fine (FG) and coarse (CG) gravels. Saturated brine is prepared from pure  $MgCl_2$  powder mixed with distilled water in plastic tank and stirred continuously.

The bentonite-aggregate mixtures ratio of 90:10, 70:30, 50:50 and 30:70 by weight ratio of bentonite.

### **1.4.3 Compaction Test**

The total compacted material mixtures of 126 specimens are under dynamic compaction with a release of weight steel hammer 10 pounds in mold of 27 times per layer in six layers of three-ring mold (Sonsakul and Fuenkajorn, 2013). The test method and calculation follow the ASTM D1557-12. The dry densities and  $MgCl_2$  brine contents are plotted to determine the maximum dry density and optimum brine content.

### **1.4.4 Direct Shear Test**

The shear strengths from the direct shear test using three-ring direct shear device are determined as the peak shear strength. The normal stress is applied by the vertical hydraulic load cell ranging from 0.2, 0.4, 0.6 to 0.8 MPa. Shear stress is applied by a horizontal hydraulic load cell. Total of 84 specimens are used. The test method and calculation follow the ASTM D3080-11. The peak shear strength is used to calculate the cohesion and friction angle.

### **1.4.5 Uniaxial Compressive Strength Test**

The uniaxial compression tests are performed on the compacted mixtures under optimum  $MgCl_2$  brine content. Neoprene sheets are used to minimize the friction at the interfaces between the loading platen and the sample surface. The axial and lateral displacements are monitored. Total of 21 specimens are used. The test method and calculation follow the ASTM D2938-95. The results are used to determine the elastic modulus and Poisson's ratio.

### 1.4.6 Swelling Tests

Comparison on the swelling capacity between the specimen mixed with  $\text{MgCl}_2$  and  $\text{NaCl}$  brines are made here. The compacted mixture under optimum brine contents is used in the swelling test. The results are used to determine the swelling capacity of backfill materials.

#### 1) Swelling tests under different bentonite weight ratios

The weight ratios of bentonite-coarse gravel from 30:70, 50:50, 70:30 and 100:0 are studied. The measurements are made for 30 days. Total of 8 specimens are used.

#### 2) Swelling tests under different aggregate types

The mixture of bentonite-aggregates of 30:70 are compacted using sludge, sand, crushed salt, fine and coarse gravels.

#### 3) Swelling under vertical stress tests

The compacted mixture is swelled under vertical stresses of 20, 50 to 100 kPa to determine the swelling capacity under vertical stresses. The test method and calculation follow the ASTM D4546-08 standard practice.

### 1.4.7 Scanning Electron Microscope Analysis

The microstructures of compacted specimens under optimum  $\text{MgCl}_2$  and  $\text{NaCl}$  brine contents are observed using scanning electron microscope (SEM). Each mixture is scanned before and after the swelling test. The effect of swelling behavior can be revealed microscopically.

#### **1.4.8 Discussions and Conclusions**

Discussions are made on the reliability and adequacies of the approaches used here. Future research needs are identified. All research activities, methods, and results are documented and compiled in the thesis. The research or findings are published in the conference proceedings or journals.

#### **1.4.9 Thesis Writing**

All research activities, methods, and results are documented and compiled in the thesis. This study can be applied to design mine backfill which mixture strength parameters of direct shear and uniaxial compressive strength tests. The findings will be published in the conference proceedings or journals.

### **1.5 Thesis Contents**

**Chapter I** describes the background of problems and significance of the study. The research objectives, methodology, scope and limitations are identified. **Chapter II** summarizes the results of the literature review. **Chapter III** describes the sample and mixture preparations. **Chapter IV** describes the results from the laboratory experiments. **Chapter V** observe the free swelling behavior of sample with bentonite weight ratios, and the swelling capacity of bentonite under vertical stress changes. **Chapter VI** describes the influence of  $MgCl_2$  and  $NaCl$  brines on the microstructures of compacted bentonite. **Chapter VII** discusses and concludes the research results and provides recommendations for future research studies.

## **CHAPTER II**

### **LITERATURE REVIEW**

#### **2.1 Compaction Test of Backfill Materials in Salt and Potash**

##### **Openings**

Ran and Daemen (1995) investigate compaction properties of crushed rock salt as a function of particle size, size gradation, compaction energy and moisture content, to determine the optimum size gradation for the highest compaction. The results indicate that compaction increases with maximum particle size and compaction energy, and varies significantly with particle size gradation and water content until the optimum water content is reached (5%), and decreases with further water content increases.

Charlermyanont and Arrykul (2005) study compaction test to determine the optimum water content and maximum dry density of compacted sand-bentonite mixtures. The results indicate that the dry unit weight of the sand-bentonite mixture increases with increasing water content. After the optimum water content is reached, the dry unit weight decreases with further increase of water content. The maximum dry unit weights and corresponding optimum water contents are obtained graphically from the peak of compaction curves. As expected, when more bentonite is added, optimum water content increased and maximum dry unit weight decreased. When more water is added after optimum water content, the dry unit weight of the compacted sand-bentonite mixtures drastically decreased, particularly at high bentonite contents. The results agree with those of Kaya and Durukan (2004) and Zhang et al. (2012).

Shariatmadari et al. (2011) investigate the effect of three different inorganic salt solutions on the compaction characteristics of two types of clay-bentonite mixtures. The three different inorganic salt solutions used are: sodium chloride (NaCl), calcium chloride (CaCl<sub>2</sub>) and Magnesium chloride (MgCl<sub>2</sub>). Bentonite clay in two proportions of 10% and 20% by weight are added to a clay soil with low plasticity. In these tests, distilled water is used as the reference liquid and salt solutions (at four concentrations varying between 0.01 and 2 N) are used as permeant liquids. Salt solution increases the maximum dry density and decrease the optimum water content of mixtures. Higher cation valance leads to higher increase in the maximum dry density and higher decrease in optimum water content as well (Figure 2.1). The reason is by adding salt to the pore fluid, the thickness of diffuse double layer decreases, therefore using the same amount of compaction energy, the particles pack better together and the dry density increases.

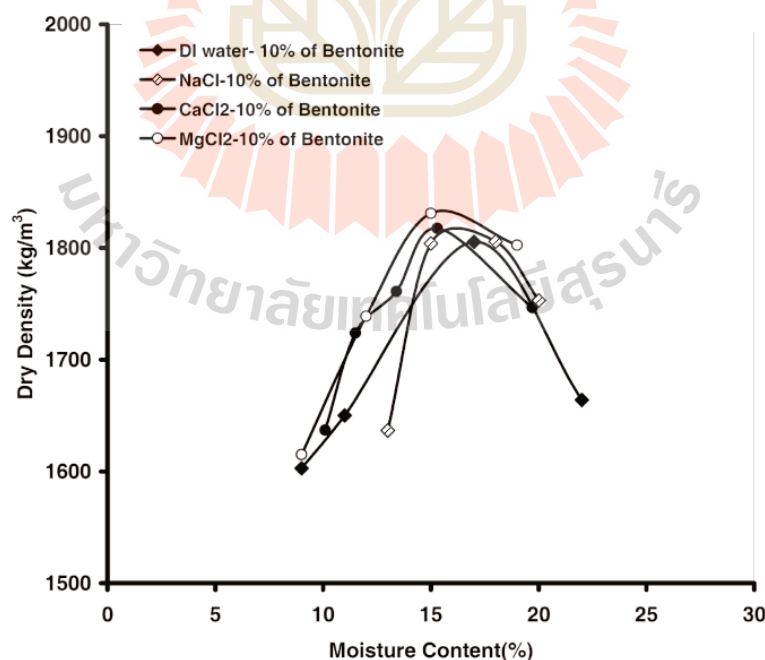


**Figure 2.1** Effect of cation valance on the maximum dry density and optimum water content (Shariatmadari et al., 2011).

Lim et al. (2013) state that sodium bentonite indeed is better than calcium bentonite in terms of functionality as electrical grounding improvement material (GIM). For most of the applications, Sodium bentonite is preferred over calcium bentonite due to its superior swelling capacity as well as its extremely low hydraulic conductivity to water.

Sonsakul and Fuenkajorn (2013) develop the three-ring compaction and direct shear testing device to determine the optimum water content, maximum dry density and shear strength of compacted soil samples. The compacted bentonite is dynamic compaction with a release of weight steel hammer 10 pounds in mold of 27 times per layer in six layers of three-ring compaction test. Compaction energy of three-ring mold is  $2,700 \text{ kN/m}^3$ , as modified proctor test. Figure 2.2 shows the three-ring mold which serves as both compact mold and shear box. The problem of sample disturbance which sometimes occurs in the standard testing is eliminated. The three-ring mold allow testing the soil with the maximum particle sizes up to 10 mm.

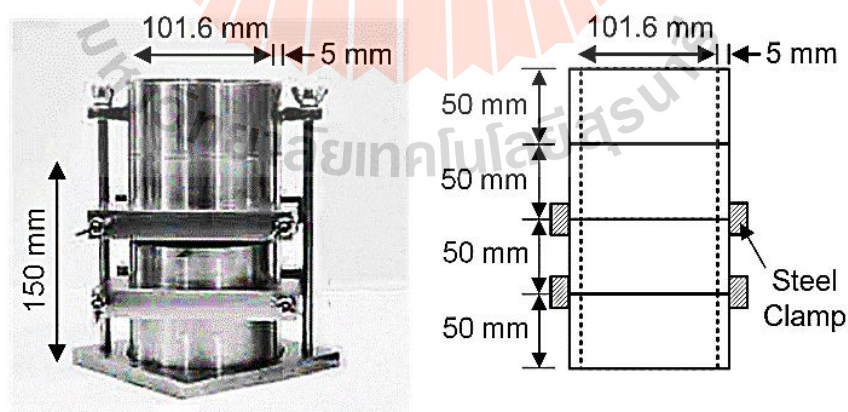


**Figure 2.2** Three-ring mold (Sonsakul and Fuenkajorn, 2013).

Proia et al. (2016) study bentonite-sand mixture, prepared with various proportions of its components. By analyzing the results of the compaction test different structure type are identified depending on the bentonite content. For a small amount of bentonite, the mixture keeps the properties of granular soils, while for higher bentonite contents there is a gradual transition to the typical mechanical behavior of plastic clay. The interaction between bentonite and sand is investigated by Scanning Electron Microscope (SEM). Figure 2.3 show the bentonite particles adhere to the sand grains surface forming “bridges” between the coarse particles. Contents of bentonite larger than 7-10% tend to interact with the sandy structure disturbing its fabric and affecting its arrangement.

Srikanth and Mishra (2016) investigate the effect of sand content of a particular size on the behavior of sand–bentonite mixture in different proportions. Various mixtures of fine sand (FS)–bentonite and medium sand (MS)–bentonite are prepared by varying the sand content from 50 to 90 % by dry weight of the mix. Results indicated that for the same proportion, the FS-bentonite and MS-bentonite mixture exhibited different optimum moisture content and maximum dry density value

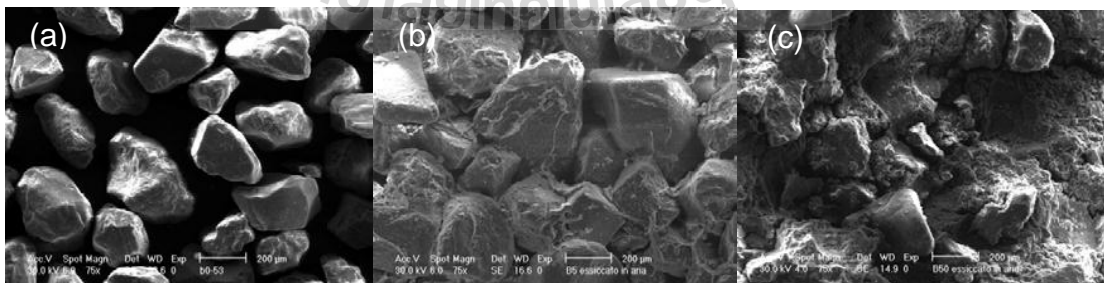


**Figure 2.3** SEM on are dried samples at magnification factors of 75x; a) sand 100%,  
b) bentonite 5% and c) bentonite 50% (Proia et al., 2016).

indicating a possible influence of sand particle size on the compaction characteristics of the mixtures. Mixtures with MS resulted in relatively a higher maximum dry density and lower optimum moisture content values for both the bentonites which can be attributed to the effective filling of the bentonite particle in the void spaces formed between the sand particles.

## 2.2 Direct Shear Test

The influence of salt solution concentration on the shear strength of bentonite-sand is studied by Zhang et al. (2016). Their test results indicate that the shear strength or shear resistance has a noticeable improvement with the increase of salt solution concentration. The test results of GMZ07 bentonite reveal that friction angle increases fairly with the salt solution concentration but the cohesion intercept doesn't. According to Di Maio and Scaringi (2016) who compact bentonite with distilled water and with NaCl solutions at various concentrations. The solution-saturated specimens are submitted to shear tests under constant driving shear stresses lower than the residual strength obtained with the salt solutions and higher than the residual strength obtained with distilled water.

The effects of particle shape and size distribution on the constitutive behavior of composite soils with a wide range of particle size are investigated by Yanrong (2013). Two comparable sets of specimens are prepared: (1) mixtures of fines (clay and silt) and an ideal coarse fraction (glass sand and beads), and (2) mixtures of fines and natural coarse fraction (river sand and crushed granite gravels). An increased coarse fraction leads to an increase in constant volume shear strength. In addition, increasing elongation or decreasing convexity of the coarse fraction increases the constant volume

friction angle. The overall roughness of the shear surface at constant volume state is negatively related to particle smoothness (convexity) and positively related to the area of the shear surface occupied by particles with particular shapes. Two parameters, convexity and elongation, derived from 2D images of the soil particles are used to quantify the particle shape. As shown in Figure 2.4.

Sonsakul et al. (2013) study shear strength of compacted bentonite-crushed salt seals between three-ring mold and ASTM standard mold. The compaction results of bentonite-crushed salt from the two technical are very similar, as shown in Figure 2.5. The direct shear test results by using both the three-ring mold and the ASTM standard test mold indicate that the three-ring test mold gives higher shear strength values for all tested. The cohesion and friction angles obtained from the three-ring mold are about 10% greater than those from ASTM standard mold. The results confirm with Pongpeng et al. (2017) who compares the compaction of bentonite-crushed salt and bentonite-gravel materials. The test results from three-ring mold are greater than those from ASTM standard mold.

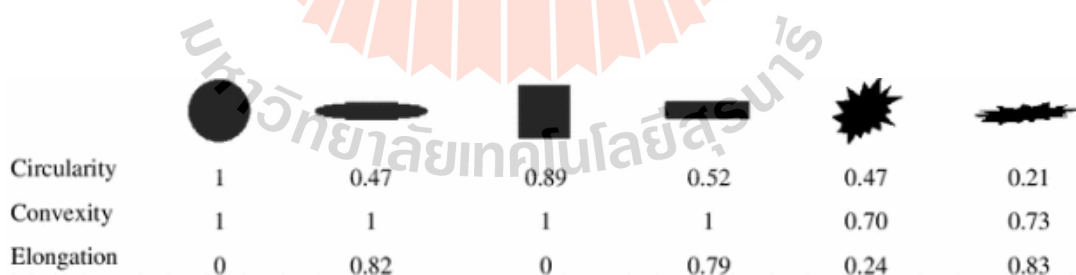


**Figure 2.4.** Illustration of particle shape parameters (Yanrong, L., 2013).

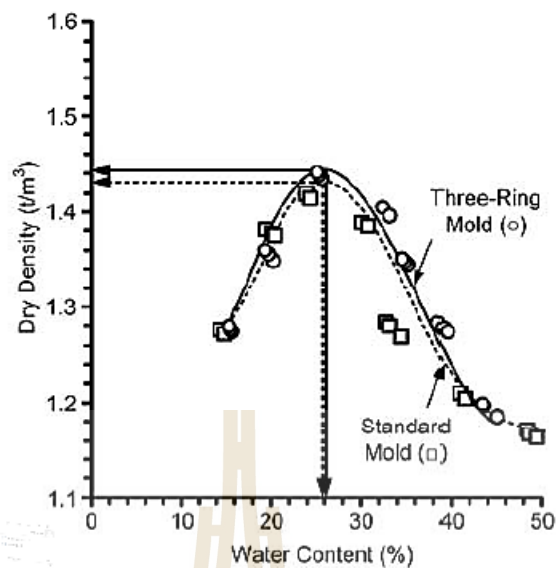


**Figure 2.5** Maximum dry density and optimum water content of bentonite obtained from three-ring mold and ASTM standard mold (Sonsakul et al., 2013).

The direct shear tests of the compacted bentonite-crushed salt and sludge-crushed salt are determined by Niewphueng and Fuenkajorn (2015) and Sattrra and Fuenkajorn (2015). The results indicate that the compacted mixtures with higher crushed salt contents show greater shear strength. The friction angle and cohesion of compacted mixtures increase with increasing crushed salt content. The friction angles and cohesion tend to be independent of the salt content. Results from the bentonite-crushed salt give lower friction angles and higher cohesion than those mixed with the sludge-crushed salt.

The coarse-grained soil properties by direct shear test on reduced-particle-size samples, and present relationship between shear strength and particle size. The larger the maximum particle size leads to the larger the shear strengths. The value of shear parameter depends on the size of grains, as the value of friction angles increases with

increasing of grain size (Bagherzadeh-Khalkhali and Mirghasemi, 2009; Soltani-Jigheh and Jafari, 2012; Kim and Ha, 2014).

Vangla and Latha (2015) study the effects of size and gradation of sand particles on the shear behavior. It is observed from the symmetric direct shear tests that the particle size has no effect on the peak friction angle when the tests are carried out at same void ratio. However, ultimate friction angles are affected by the particle size. Ultimate friction angle increases with the increasing particle size. Figure 2.6 show that the stress–strain response of the sands is influenced by the angularity and increasing angularity results in higher peak shear strength due to increase in interlocking forces. The angularity and roundness properties of the sands are almost same in the present study, indicating that the effect of morphology is masked and the variations in the shear behavior are only due to the particle size effects. According to Holtz and Kovacs (1981) particle size does not have any effect on the peak friction angle ( $\phi_p$ ) if the void ratio is same.

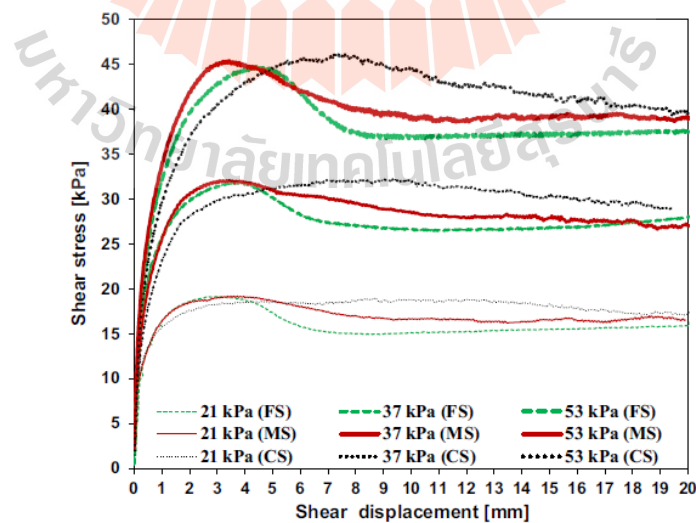


**Figure 2.6** Shear stress versus shear displacement response of different sands (Vangla and Latha, 2015).

### 2.3 Swelling Test

Swelling characteristics are considered the key property correlating with the expected functionality of a buffer/backfill material. Many researchers have studied the swelling characteristics of bentonite and bentonite–sand mixtures. Several attempts have been made by earlier researchers to obtain time-swelling relationships for swelling bentonite. Cui et al. (2012) report that swelling deformation tend to be independent of the sand content. With the increase of the sand content ratio, the maximum swelling pressure presents an exponential decrease, and the maximum swelling strain decreases, expressing a quadratic curve. This means that increasing sand content ratios can restrain the swell characteristics of the GMZ bentonite-sand mixtures.

Borgesson et al. (2003) present the mixtures of 10% and 30% bentonite have a much higher measured swelling pressure than expected, which means that the homogeneity is poor, since the clay density of the filled pores must be much higher and thus yield a much higher swelling pressure. It seems the limit where the backfill will be inhomogeneous is between 30% and 50% bentonite content. 30:70 seems though to be a good combination since the measured swelling pressure is higher and the measured hydraulic conductivity only slightly higher than the theoretical values for an ideally homogeneous material.

Mašín and Khalili (2015) study the swelling characteristics of bentonite under loading conditions. At the same vertical pressure, a higher dry density results in a larger final swelling pressure. For the specimens with the same dry density, the swelling pressure and vertical pressure have a decreasing linear relation in their logarithmic scales, as shown in Figure 2.7.

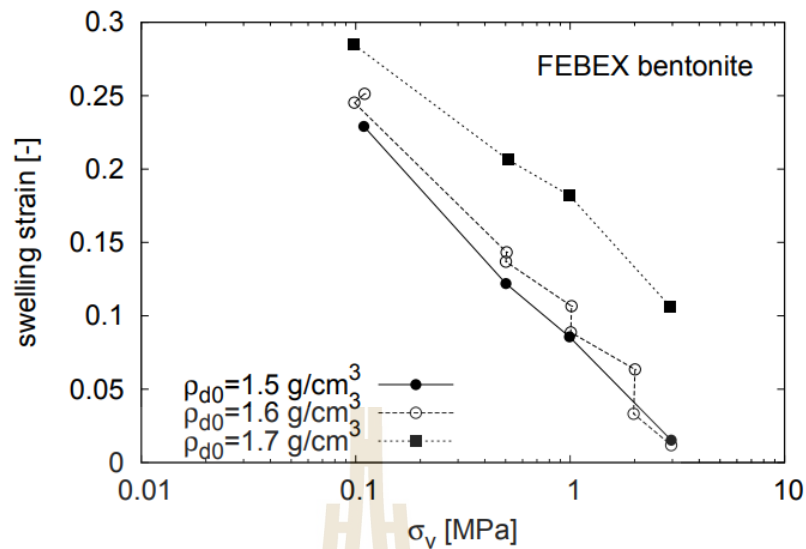


**Figure 2.7** Swelling pressure and vertical pressure relation from constant stress tests (Mašín and Khalili, 2015).

Agus et al. (2010) study the suction characteristics of bentonite–sand mixtures containing different proportions of bentonite. Total suction is shown to be primarily a function of water content and bentonite content. The higher the percentage of bentonite in the mixture, the higher the total suction for the same water content. It is reasonable to assume that water is only absorbed by the bentonite. The difference in the total suction for different water content at the same mixture bentonite content indicated that suction can decrease with increasing water content.

Chun-Ming et al. (2013) investigate salinity effects of infiltrating solutions on swelling pressure and hydraulic conductivity. The swelling pressure of compacted GMZ01 bentonite hydrated with NaCl solutions is lower than that with CaCl<sub>2</sub> solutions. The difference depends on the concentration of solutions. For low concentrations of salt solutions, the difference is small. On the contrary, for higher concentrations, the swelling pressure with the low-valence salt (NaCl) solutions is much lower than that

with high-valence salt ( $\text{CaCl}_2$ ) solutions. This phenomenon suggests that the weakening effect of  $\text{Na}^+$  on swelling pressure is greater than that of  $\text{Ca}^{2+}$ . Results obtained show that the swelling pressure of GMZ01 bentonite decreases with increasing concentration of infiltrating solutions, while the degree of the impact decreases with the increase of concentrations. Moreover, swelling pressure reaches stability more rapidly in case of high concentrations. This observation can be explained by the swelling process of compacted bentonite described in Figure 2.8. Commonly, swelling of bentonite exposed to water or electrolytes is primarily on account of two mechanisms: the crystalline swelling and the diffuse double-layer swelling (Madsen, 1989; Savage, 2005). The crystalline swelling is caused by the hydration of exchangeable cations ( $\text{K}^+$ ,  $\text{Na}^+$ ,  $\text{Ca}^{2+}$  and  $\text{Mg}^{2+}$ ) between montmorillonite unit layers that have a structure with one alumina octahedral sheet sandwiched between two silica tetrahedral sheets. After the adsorption of maximum number of hydrates, surface hydration becomes less significant and diffuse double-layer repulsion becomes the governing swelling mechanism.

Chen et al. (2016) study the one-dimensional swelling tests on compacted GMZ bentonite with NaCl solution 0, 0.1, 0.5, 1.0 mol/L under three vertical stresses of 0.06, 0.062 and 0.82 MPa. The results indicate that for all concentrations, the total vertical swelling strains decreased with increasing vertical stress. Under the same vertical stress, the swelling strain decreases with increasing concentration. It can be also observed from Figure 2.9. This observation is in accordance with the results reported by Studds et al. (1998) and Navarro et al. (2017) who observed that the vertical swelling strains of compacted bentonite-sand decreased with the increase in salt concentration of NaCl solution.

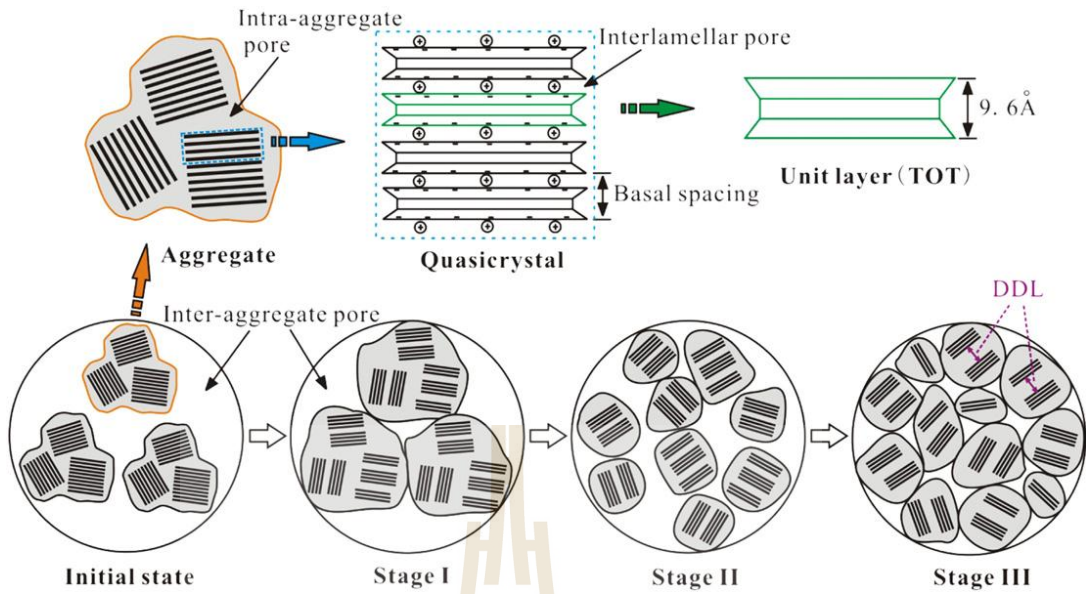


**Figure 2.8** Conceptual diagrams of constant-volume swelling process and microstructure of compacted GMZ01 bentonite (Villar, 2002; Suzuki et al., 2005).

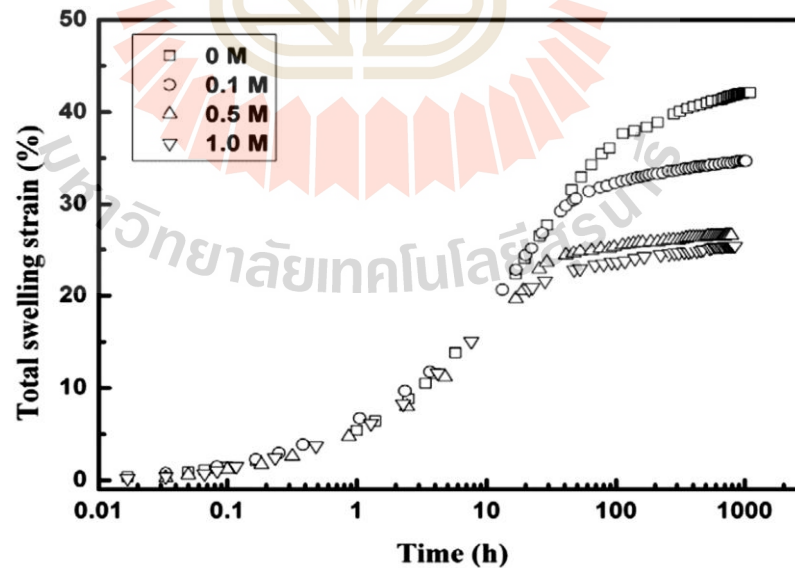


**Figure 2.9** Swelling test with various NaCl solutions (0, 0.1, 0.5, 1.0 mol/L) under vertical stress of 0.06 MPa (Chen et al., 2016).

## 2.4 Effect on Hydraulic Conductivity

Studds et al. (1998) study the hydraulic conductivity of Na bentonite powder and bentonite sand mixtures (10 and 20% of bentonite by dry weight) have been measured with distilled water and various salt solutions like Na, K, Cs, Mg, Ca and Al chloride solutions at 0.01, 0.1 and 1 mol/l concentration. The hydraulic conductivity of a bentonite sand mixture to aqueous solutions can be predicted from the hydraulic conductivity of the bentonite in the appropriate solution and the porosity and tortuosity of the sand matrix the hydraulic conductivity of a mixture decreases as  $w_t\%$  clay decreases, hydraulic conductivity of each mixture increases as the clay-void ratio increases.

Frankovská et al. (2010) study the effect of NaCl on hydraulic properties of Bentonite and bentonite – palygorskite mixture. The purpose of this work is to investigate the properties of Na bentonite and bentonite–palygorskite filler material for GCL in saline solutions in the range between 0.5% and 10% (0.09 and 1.8 M) NaCl concentration. The investigation has been carried out to evaluate and study the chemical and geotechnical properties of Na-bentonite and bentonite–palygorskite mixture. The observations suggest that the resistance of Na-bentonite to chlorides is increased by adding 40% palygorskite Hydraulic conductivity is determined for water and for 10% NaCl (1.80 M) solution. The results show that Na-bentonite palygorskite mixture serves as an effective absorber of both water and saline solutions up to a concentration of 10% (1.80 M) of NaCl without increasing the hydraulic conductivity.

Cho et al. (2011) study the influence of water salinity on the hydraulic conductivities of compacted bentonites with several dry densities. The results showed that the hydraulic conductivity increases with increasing salinity only when the dry

density of bentonite is relatively low. The degree of increase becomes more remarkable at a lower dry density of bentonite. For bentonite with the density of  $1.0 \text{ Mg/m}^3$  and  $1.2 \text{ Mg/m}^3$ , the hydraulic conductivity of the  $0.4 \text{ M NaCl}$  solution increases up to about 7 times and 3 times, respectively higher than that of freshwater. However, for the bentonite with a dry density higher than  $1 \text{ Mg/m}^3$ , the salinity has an insignificant effect on the hydraulic conductivity, and the hydraulic conductivity is nearly constant within the salinity range of  $0.04$  to  $0.4 \text{ M NaCl}$ . The pre-saturation of the bentonite specimen with freshwater has no significant influence on the hydraulic conductivity.

## 2.5 Consolidation Test of Backfill Materials

Butcher (1993) concludes that a 70% by weight salt and 30% by weight bentonite mixtures is preferable to pure crushed salt as backfill for disposal rooms in the Waste Isolation Pilot Plants. The real advantage of the salt/bentonite backfill depends, therefore, on bentonite potential for absorbing brine and radionuclides are shown in Table 2.1.

Zhang et al. (2016) investigate the effects of salt solution concentration on mechanical behavior and microstructural features of a sodium bentonite (GMZ07 bentonite) and its mixture with sand saturated with distilled water and sodium chloride solutions at different concentrations ( $0.2$ ,  $0.5$  and  $1.0 \text{ mol/L}$ ) are consolidated to a specified stress. The results are obtained from consolidation test of GMZ07 bentonite by distilled water and NaCl solution with the concentration of  $0.5 \text{ mol/L}$ . The result indicated that the consolidation of GMZ07 bentonite by distilled water is longer than by NaCl solution, as shown in Figure 2.10.

**Table 2.1.** Comparison of the properties of crushed-salt and salt/bentonite backfill  
(Butcher, 1991)

<b>Criteria</b>		<b>Crushed-Salt Backfill</b>	<b>Salt/Bentonite Backfill</b>
<b>Required Criteria</b>	Low Permeability	$< 10^{-19} \text{ m}^2$	$< 10^{-19} \text{ m}^2$
	Low Porosity	$< 0.08$	$< 0.13$
	Chemical Stability	Greatest	Good
	Shear Strength	Acceptable	Acceptable
	Ease of Emplacement	Good	Good
<b>Desirable Criteria</b>	Effect of additives on Consolidation	Predictable	Predictable
	Brine Sorption	None	Questionable
	Radionuclide Sorption	None	Good
	Deformability, Ability to Fill Voids	Excellent	Excellent
	Thermal Conductivity	Acceptable	Acceptable

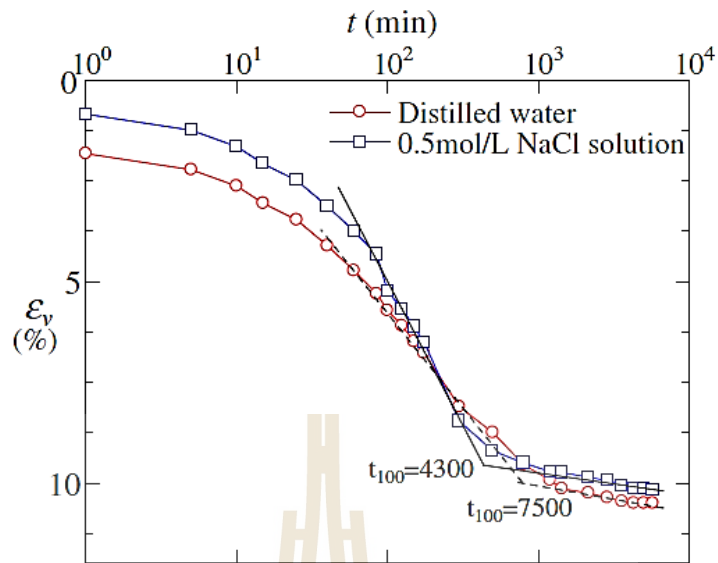


**Figure 2.10** Consolidation curve of GMZ07 bentonite by distilled water and 0.5 mol/L NaCl Solution (Zhang et al., 2016).

Khamrat et al. (2018) study the consolidation test on crushed salt mix with NaCl solution, and Suwannabut et al. (2018) there are similar tests. But there is a replacement of the solution by used to  $MgCl_2$ . Under axial stresses ranging from 2.5 to 10 MPa for 3-180 days are compared (Figure 2.11). At the same solution, the results indicate that higher applied consolidation stress ( $\sigma_{cons}$ ) leads to a larger strain. The strain rates decrease with time, and tend to remain relatively constant after 30 days. The uniaxial compression tests with larger consolidation period and stress show higher strength and elasticity of the specimen, while Poisson's ratio decreases slightly. NaCl solution tends to higher uniaxial compressive strength than those the  $MgCl_2$  solution due to  $MgCl_2$  solution does not have recrystallization of the salt particles.

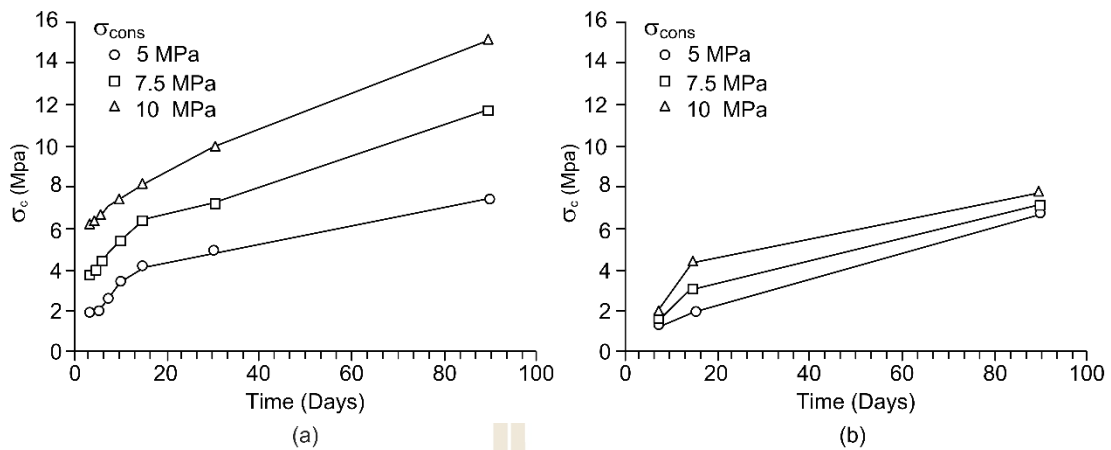


**Figure 2.11** Consolidation crushed salt with NaCl solution (a) (Khamrat et al., 2017) and with MgCl<sub>2</sub> solution (b) (Suwannabut et al., 2018).

Theerapun et al. (2017) study the effects of halite, carnallite and magnesium brines on the time-dependent deformation of salt and potash specimens by uniaxial creep test. The specimens are submerged in saturated brine prepared from halite, carnallite and magnesium chloride. The creep testing results indicate that the creep rate of salt specimens are not affected by the halite, carnallite and magnesium brines, no change in creep rate is detected before, during and after brine submersion. The potash specimens however fail after submersion under halite and carnallite brine, probably because the specimen can dissolve in these solutions, and hence accelerates the creep rate and eventually reaches the tertiary creep phase (toward failure). Under saturated magnesium brine, the creep rates of the potash specimens remain constant before, during and after brine submersion. This suggests that all three solutions can be used in salt mines, while magnesium chloride solution is suitable for potash mines.

# **CHAPTER III**

## **TESTING MATERIALS**

### **3.1 Introduction**

This chapter describes basic characteristics of testing materials and sample preparation to obtain the optimum brine content, dry density, shear strength and compressive strength of compacted mixtures.

### **3.2 Test Materials**

The aggregates used in this study include sludge, sand, crushed salt, fine and coarse gravels. The construction grade bentonite is used to mix with each type of the aggregates. The chemical compositions of the bentonite and sludge are determined by X-Ray fluorescence (XRF), as shown in Table 3.1.

#### **3.2.1 Sieve analysis**

Grain size analysis is performed to determine the percentage of various particle sizes (Figure 3.1). The sources of materials are described as follows:

- Bentonite used in this study is from Thai Nippon Chemical Industry Co., LTD, Thailand. It has particle sizes ranging from 0.425 to 0.075 mm.
- Sludge obtained from dewatering plant of Bang Khen Water Treatment Plant located in Bangkok Metropolis. The particle sizes are less than 0.075 mm.
- Crushed salt is prepared from Middle member of the Maha Sarakham formation, northeastern Thailand. The salt is crushed by hammer mill

**Table 3.1** Chemical compositions of the tested bentonite and sludge.

Compositions	Weight (%)	
	Bentonite	Sludge
SiO <sub>2</sub>	48.272	52.37
Al <sub>2</sub> O <sub>3</sub>	12.776	23.47
Fe <sub>2</sub> O <sub>3</sub>	27.403	6.33
Na <sub>2</sub> O	1.232	0.22
MgO	1.869	0.96
CaO	N/D	0.79
K <sub>2</sub> O	1.806	1.55
TiO <sub>2</sub>	4.622	0.79
P <sub>2</sub> O <sub>5</sub>	1.404	0.34
SO <sub>3</sub>	0.091	0.55
MnO	0.263	0.22
CuO	0.018	0.01
Rb <sub>2</sub> O	N/D	0.01
SrO	N/D	0.01
Y <sub>2</sub> O <sub>3</sub>	N/D	<0.01
ZrO <sub>2</sub>	N/D	0.03
Nb <sub>2</sub> O <sub>5</sub>	N/D	<0.01
BaO	N/D	0.01
CeO <sub>2</sub>	N/D	N/D
Cr <sub>2</sub> O <sub>3</sub>	0.018	0.02
Cl	0.087	0.07
Co <sub>3</sub> O <sub>4</sub>	0.071	N/D
NiO	0.022	N/D
CeO <sub>2</sub>	0.047	N/D
Total	100	100

N/D = not detected

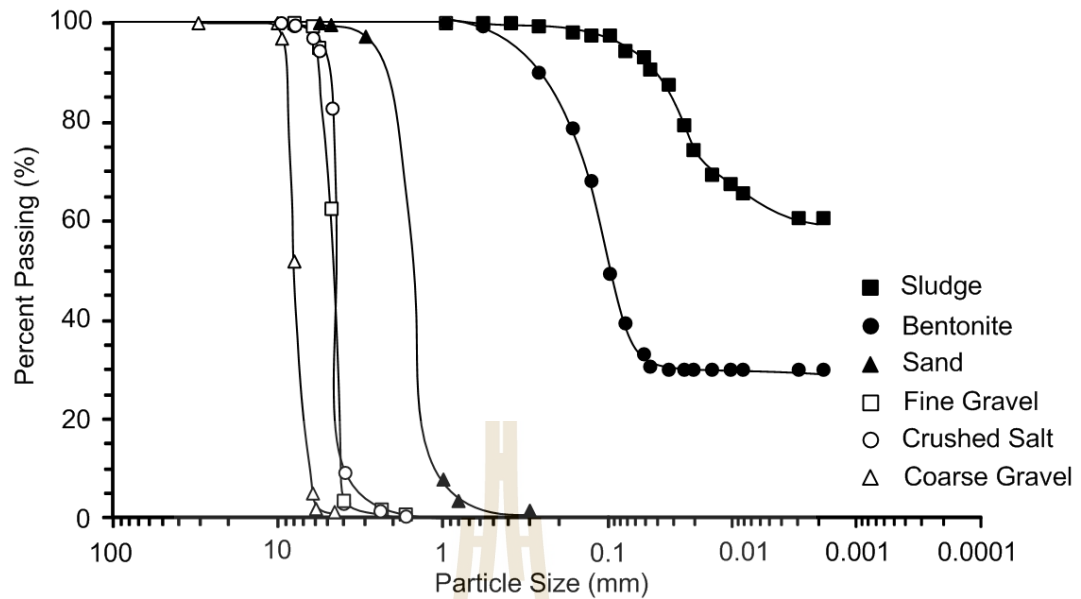


**Figure 3.1** Particle size distributions of tested materials.

to obtain grain sizes ranging from 4 to 6 mm. This size range is equivalent to that expected from the mine processing plant.

- Sand and fine and coarse gravels are collected from Khok Kruat District, Nakhon Ratchasima Province. It has particle sizes ranging from 1-2, 4-6, 6.35-9.53 mm, respectively.

### 3.2.2 Unified soil classification system

The classification criteria are in accordance with the Unified Soil Classification System. Classification of fine grain soil (50% or more passes the No.200 sieve) by using Atterberg's Limits. The results are listed in Table 3.2. The bentonite and sludge are sandy elastic silt (MH) and silt (ML), respectively.

**Table 3.2** Classification of bentonite and sludge.

Property		Bentonite	Sludge
Liquid limit	(%)	79.86	41.24
Plastic limit	(%)	36.46	26.61
Plasticity index	(%)	43.40	14.63
Type of material		Sandy elastic silt (MH)	Silt (ML)

To classify the crushed salt, sand and gravel in accordance with ASTM (D2487-06) the uniformity coefficient ( $C_u$ ) and the coefficient of curvature ( $C_c$ ) are determined as follows:

$$C_u = D_{60}/D_{10} \quad (3.1)$$

$$C_c = D_{30}^2 / (D_{10} \times D_{60}) \quad (3.2)$$

where  $D_{60}$  is particle size at 60% finer,  $D_{30}$  is particle size at 30% finer and  $D_{10}$  is particle size at 10% finer. The uniformity coefficient and the coefficient of curvature for materials are shown in Table 3.3. The crushed salt and Fine gravel are poorly graded sand with gravel (SP). Sand is Poorly graded sand (SP) and coarse gravel is Poorly graded gravel (GP).

**Table 3.3** Classification of sand, fine and coarse gravel.

Material	$C_u$	$C_c$	Type of material
Crushed salt	1.25	0.80	Poorly graded sand with gravel (SP)
Sand	1.4	1.1	Poorly graded sand (SP)
Fine gravel	1.25	0.80	Poorly graded sand with gravel (SP)
Coarse gravel	1.23	0.13	Poorly graded gravel (GP)

### 3.2.3 Sphericity and roughness of aggregates

The sphericity and roughness are determined from individual particles using an optical microscope (Olympus BX51M), as shown in Figure 3.2. Based on the widely used classification systems given by Powers (1982) (Figure 3.3), the sand and crushed salt are classified as angular to sub-angular with spherical shape. The fine and coarse gravels are classified as sub-rounded to rounded with sub-discoidal shape. The averages of the roughness and sphericity for each material are shown in Table 3.2.





**Figure 3.2** Size and shape of tested materials.

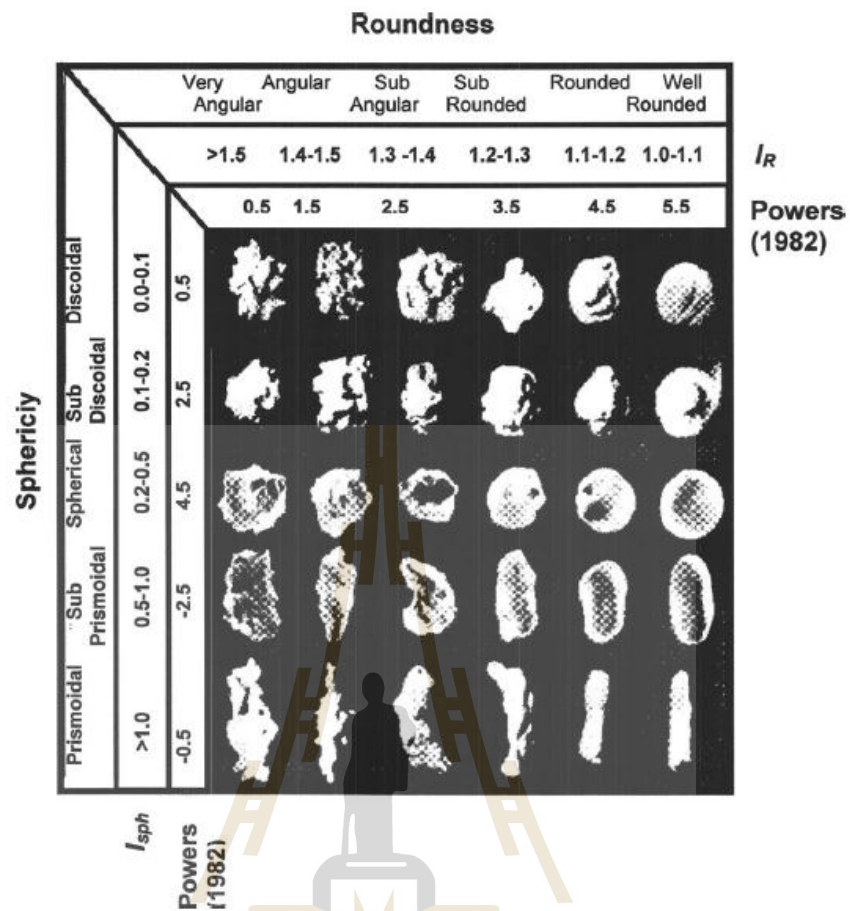


**Figure 3.3** Estimation of roundness and sphericity of sedimentary particles (Powers, 1982).

**Table 3.4** Particle shape classification of aggregates based on Powers (1982).

Aggregate	Roundness Classification		Sphericity Classification	
	Sand	1.5 - 2.5	Angular-Sub Angular	4.5
Crushed salt	1.5 - 2.5	Angular-Sub Angular	4.5	Spherical
Fine gravel	3.5 - 4.5	Sub Rounded-Rounded	2.5	Sub-Discoidal
Coarse gravel	3.5 - 4.5	Sub Rounded-Rounded	4.5	Spherical

### 3.3 Saturated MgCl<sub>2</sub> Brine

Saturated brine is prepared from pure MgCl<sub>2</sub> powder mixed with distilled water in plastic tank and stirred continuously. The proportion of MgCl<sub>2</sub> to water is 1.76:1 by weigh to obtain saturated conditions. A plastic rod is used to stir the mixture continuously for 20 minutes. The dry densities of MgCl<sub>2</sub> is 2.32 g/cc. Specific gravity of the saturated MgCl<sub>2</sub> brine is calculated as,  $S.G. = \rho_{\text{Brine}}/\rho_{\text{H}_2\text{O}}$  where  $\rho_{\text{Brine}}$  is density of saturated MgCl<sub>2</sub> brine (measured by a hydrometer in kg/m<sup>3</sup>) and  $\rho_{\text{H}_2\text{O}}$  is density of distilled water. The properties of MgCl<sub>2</sub> brine are as follows: density = 1.31 g/cc, pH = 7.1 and viscosity = 10.5 cP. The MgCl<sub>2</sub> brine is the waste product from the mine processing plant. It is used here to obtain a chemical compatibility between the mixtures and the salt and potash around the openings to be backfilled (Theerapun et al., 2017).

### 3.4 Bentonite and Aggregate Mixtures

The bentonite-aggregate (sludge, crushed salt, sand, fine gravel and coarse gravels) mixtures weight ratio are 90:10, 70:30, 50:50 and 30:70. The mixtures are prepared in plastic tray using by 2.7 kilograms. The MgCl<sub>2</sub> brine is added by spaying on the mixture until a desired brine content is reached. They are mixed thoroughly using plastic spatula.

## **CHAPTER IV**

### **LABORATORY TESTING**

#### **4.1 Introduction**

This chapter describes test apparatus, methods and results of the compaction, direct shear and uniaxial compression testing. The compaction testing is performed to obtain the maximum dry densities and optimum  $\text{MgCl}_2$  brine content. The specimens after compaction are used to determine the mechanical properties.

#### **4.2 Test Apparatus**

Three-ring mold (Sonsakul and Fuenkajorn, 2013) is used to performed the compaction test (Figure. 4.1). The inside diameter is 10.16 cm, outer diameter is 10.76 cm and combined height is 15.19 cm. It is designed to be used with a specifically-developed shear test frame for the direct shear test (Figure. 4.2). The three-ring compaction and direct shear mold has been developed to determine the optimum moisture content, maximum dry density and shear strength of compacted soil samples with particle sizes up to 10 mm. It is designed to be used as a compaction mold and direct shear mold without removing the soil sample, and hence eliminating the sample disturbance.

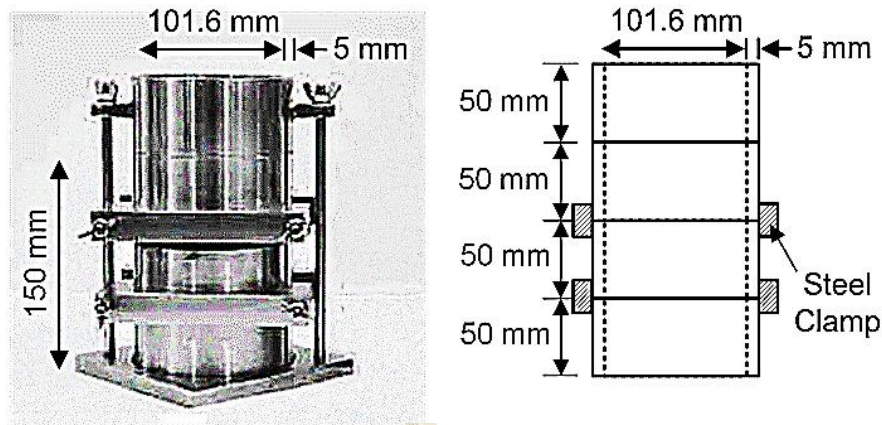


**Figure 4.1** Three-ring compaction mold (Sonsakul and Fuenkajorn, 2013).

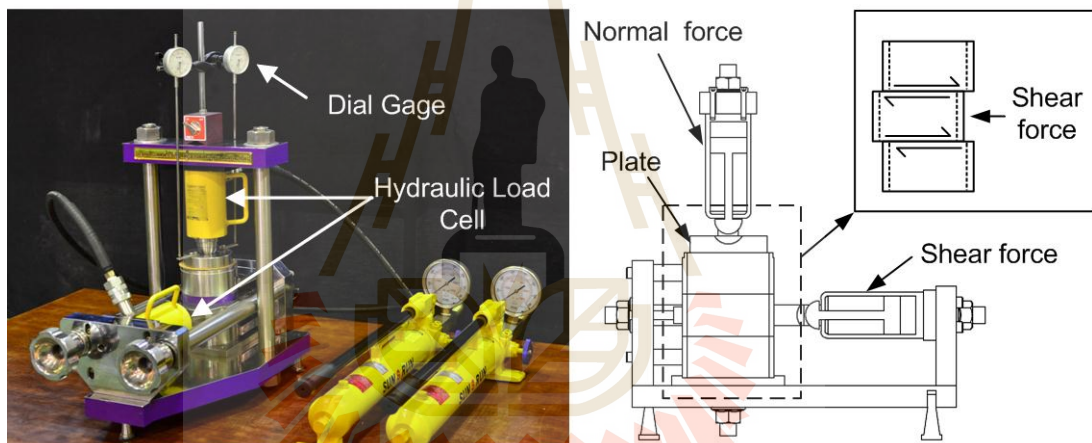


**Figure 4.2** Direct shear tests frame for three-ring mold (Sonsakul and Fuenkajorn, 2013).

## 4.3 Compaction Test

### 4.3.1 Test method

The bentonite-aggregates are mixed with the saturated  $\text{MgCl}_2$  brine using percentages of bentonite of 5, 10, 15, 20, 25 and 30% by weight. The bentonite is dynamic ally compacted with a release of weight steel hammer 10 pounds in mold of 27 times per layer for six layers in the three-ring mold. Total energy of compaction is

approximately  $2,700 \text{ kN}\cdot\text{m}/\text{m}^3$ . Energy of compaction (J) can be calculated by Proctor (1933):

$$J = \frac{n \times W \times L \times t}{V} \quad (4.1)$$

where J is compaction energy per unit volume, n is number of blows per layer, W is weight of hammer, L is height of drop of hammer, t is number of layers and V is volume of mold.

After compacted specimens are oven-dried at  $105 \pm 5^\circ \text{C}$  for 24 hours, the dry densities and brine contents are plotted to determine the maximum dry density and optimum  $\text{MgCl}_2$  brine content. The  $\text{MgCl}_2$  brine content ( $W_b$ ) can be calculated by (Fuenkajorn and Daemen, 1988):

$$W_b = \frac{[100 + SB] \times \left[ W_1 - W_2 - \left( \frac{W_i}{100} \right) (W_2 - W_{\text{can}}) \right] \times 100}{100(W_2 - W_{\text{can}}) - SB(W_1 - W_2)} \quad (4.2)$$

where  $W_b$  is  $\text{MgCl}_2$  brine content (% by weight),  $W_i$  is initial water content of specimen (% by weight),  $W_{\text{can}}$  is weight of container (g),  $W_1$  is weight of wet soil and container (g),  $W_2$  is weight dry soil and container (g) and SB (Solubility) is 176.3% by weight of  $\text{MgCl}_2$  in water.

The dry density ( $\rho_{\text{dry}}$ ) of the compacted mixtures can be calculated as:

$$\rho_{\text{dry}} = [ \rho_{\text{wet}} / (W_b + 100) ] \times 100 \quad (4.3)$$

where  $\rho_{\text{dry}}$  is dry density of compacted specimen (g/cc),  $\rho_{\text{wet}}$  is wet density of compacted specimen (g/cc),  $W_b$  is MgCl<sub>2</sub> brine content of specimen (% by weight).

#### 4.3.2 Compaction test results

A total of 26 specimens has been tested. The results show the maximum dry density ( $\rho_{\text{dry}}$ ) as a function of MgCl<sub>2</sub> brine weight ratios in Figure 4.3. The mixtures with lower bentonite contents have higher dry density than those with the higher bentonite weight ratios. This holds true for all types of aggregate. This is due to the fact that the aggregate densities are greater than that of the bentonite. Coarser aggregate particles tend to have higher dry density than those of the finer particles. The compaction curves of fine and coarse gravel under 30% of bentonite weight ratios show rapidly decrease dry densities while increase brine content after optimum brine content. Proctor (1933) states that for any increment in the water content after the “optimum water content”, the volume of voids tends to increase, and hence soil will obtain a lower density. Fine and coarse gravel are classified as poorly grade, so voids spaces will increase. Figure 4.4 shows the decrease of the maximum dry density with increasing bentonite weight ratios. The optimum MgCl<sub>2</sub> brine contents however increase with the bentonite weight ratio. The results of the compaction test are summarized in Table 4.1. This agrees reasonably well with the test results obtained by Kaya and Durakan (2004), Charlermyanont and Arrykul (2005), Soltani-Jigheh and Jafari (2012) and Zhang et al. (2012).

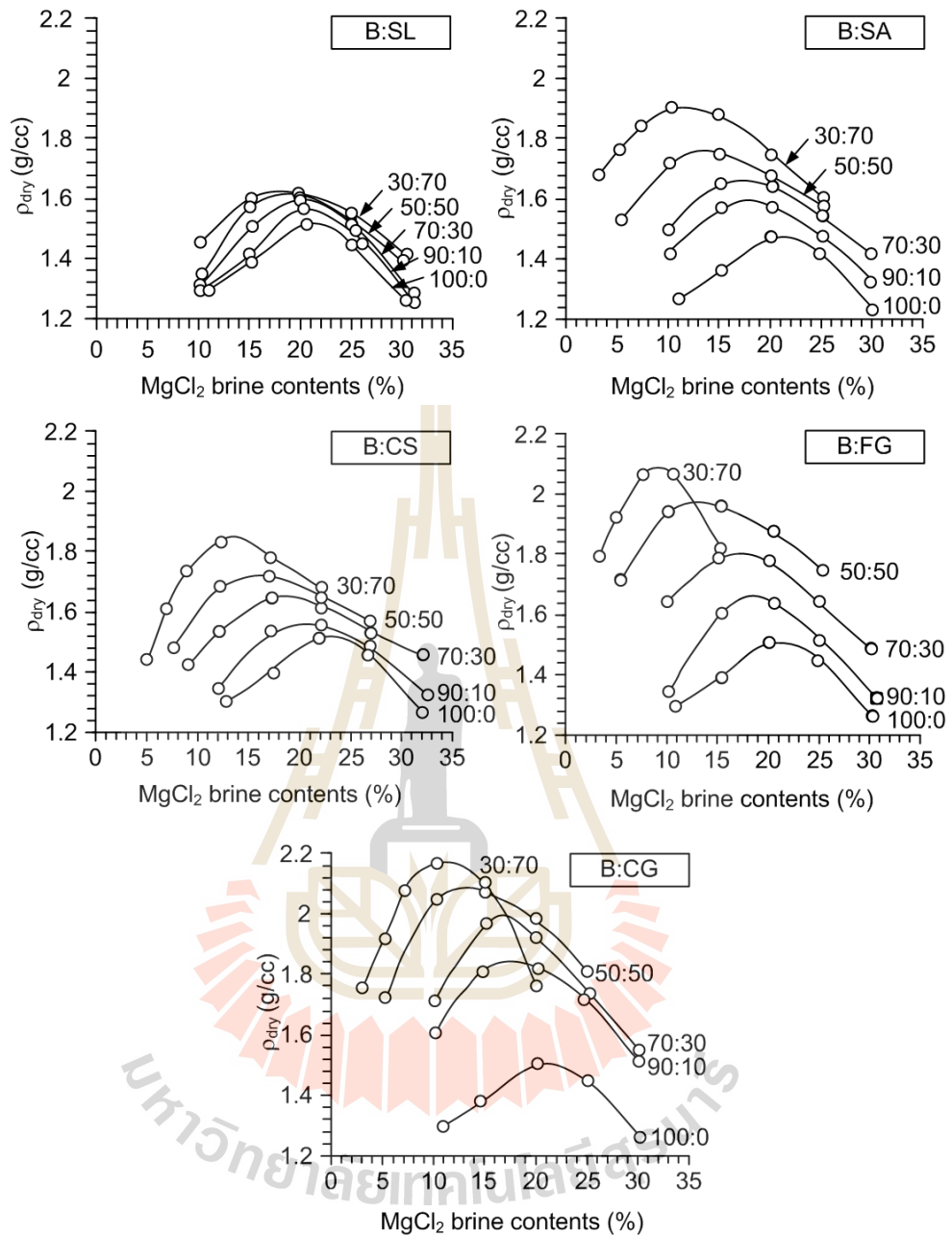


**Figure 4.3** Maximum dry densities as a function of MgCl<sub>2</sub> brine contents.

B = bentonite, SL = sludge, SA = sand, CS = crushed salt, FG = fine gravel and CG = coarse gravel.

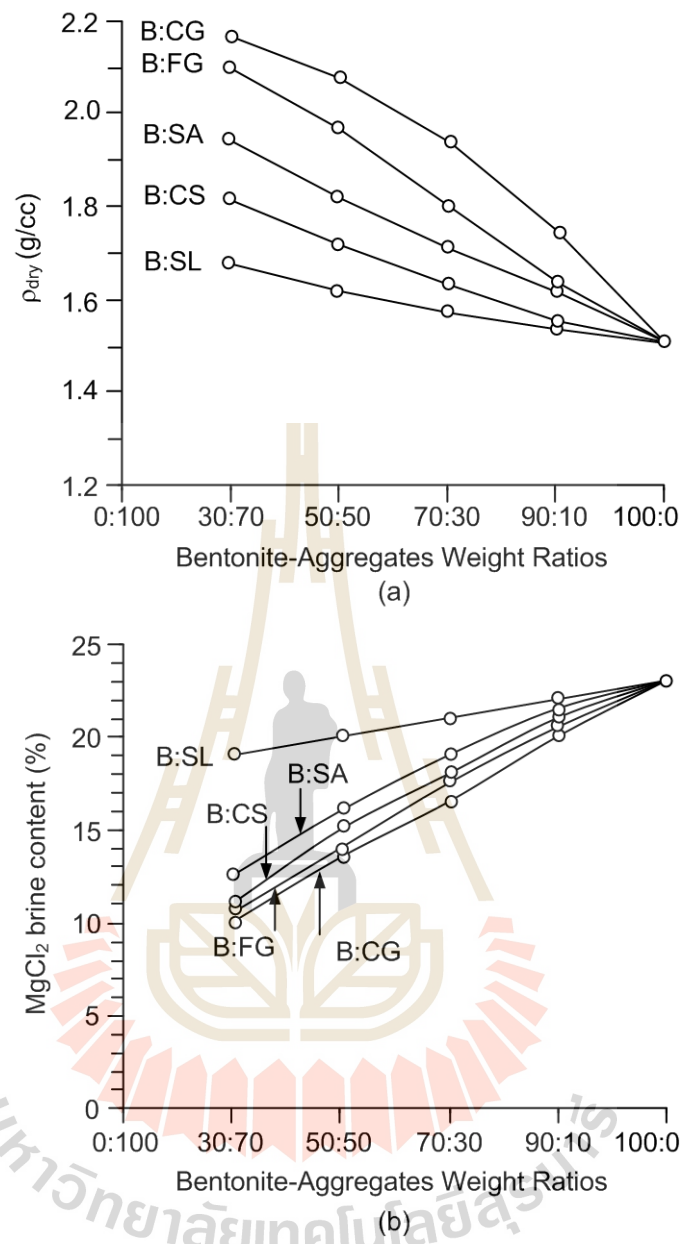


**Figure 4.4** Maximum dry densities (a) and optimum  $MgCl_2$  brine contents (b) as a function of bentonite-aggregate weight ratio.

**Table 4.1** Compaction test results.

<b>Bentonite (B) : Aggregates</b>	<b>Weight ratio</b>	<b>Maximum dry densities (g/cc)</b>	<b>Optimum MgCl<sub>2</sub> brine contents (%)</b>
Bentonite : Sludge (B:SL)	100:0	1.51	20.70
	90:10	1.54	20.25
	70:30	1.57	19.50
	50:50	1.60	18.70
	30:70	1.61	18.20
Bentonite : Sand (B:SA)	90:10	1.62	19.00
	70:30	1.69	17.00
	50:50	1.79	14.50
	30:70	1.94	12.00
Bentonite : Crushed Salt (B:CS)	90:10	1.56	18.70
	70:30	1.64	16.50
	50:50	1.72	13.80
	30:70	1.82	11.30
Bentonite : Fine Gravel (B:FG)	90:10	1.64	18.50
	70:30	1.80	16.00
	50:50	1.97	13.00
	30:70	2.09	10.50
Bentonite : Coarse Gravel (B:CG)	90:10	1.80	18.00
	70:30	1.97	15.50
	50:50	2.10	12.50
	30:70	2.16	9.80

## 4.4 Direct Shear Test

### 4.4.1 Test method

After compaction, the clamps of the three-ring mold are removed, and the mold is placed into a direct shear load frame. The lateral load system pushes the middle ring, and the vertical load system applies a constant normal stress on the compacted sample. The shear stress is applied while the shear displacement and dilation are recorded for every 0.1 mm of shear displacement. The normal stress and shear stress can be calculated from the Equations (4.4) and (4.5):

$$\sigma_n = P/A \quad (4.4)$$

$$\tau = F/2A \quad (4.5)$$

where  $\sigma_n$  is normal stress, P is normal load, A is cross section area of sample, F is shear force and  $\tau$  is shear stress.

Based on the Coulomb criterion the cohesion and friction angles of the compacted mixtures under their optimum  $MgCl_2$  brine content can be calculated from equation:

$$\tau = c + \sigma_n \tan \phi \quad (4.6)$$

where  $\tau$  and  $\sigma_n$  are the shear strength and normal stress,  $\phi$  is the angle of friction, and c is cohesion.

#### 4.4.2 Direct shear test results

The shear stresses as a function of shear displacement are shown in Figures 4.5 through 4.9. The shear stresses increase with shearing displacement, particularly under high normal stresses. The dilations ( $d_n$ ) tend to increase with the shearing displacement ( $d_s$ ). The amount of dilation significantly increases as the particle size of aggregates increases. Figure 4.10 shows the shear strength and normal stress curves. For all mixtures the shear strength increases linearly with the normal stress. The compacted mixtures with smaller particles show greater shear strengths than those with the larger ones. The cohesions and friction angles of the compacted mixtures are plotted in Figure 4.11. It is clear that increasing the bentonite weight ratio significantly decreases the cohesions ( $c$ ) and friction angles ( $\phi$ ) of the mixtures. The  $c$  and  $\phi$  also depend on particle shape. The mixtures with angular shape (crushed salt) tend to show larger  $c$  and  $\phi$  values, as compared to those with the rounds shape (fine gravel). The cohesion of coarser mixing particles (e.g. gravel and crushed salt) is lower than those of the finer particles (e.g. sludge). The friction angle of coarser particles is however higher than that of the finer particles. This may be due to the greater frictional resistance of the grain surfaces for the coarse materials. Table 4.2 shows the cohesion and friction angle obtained from the direct shear testing.

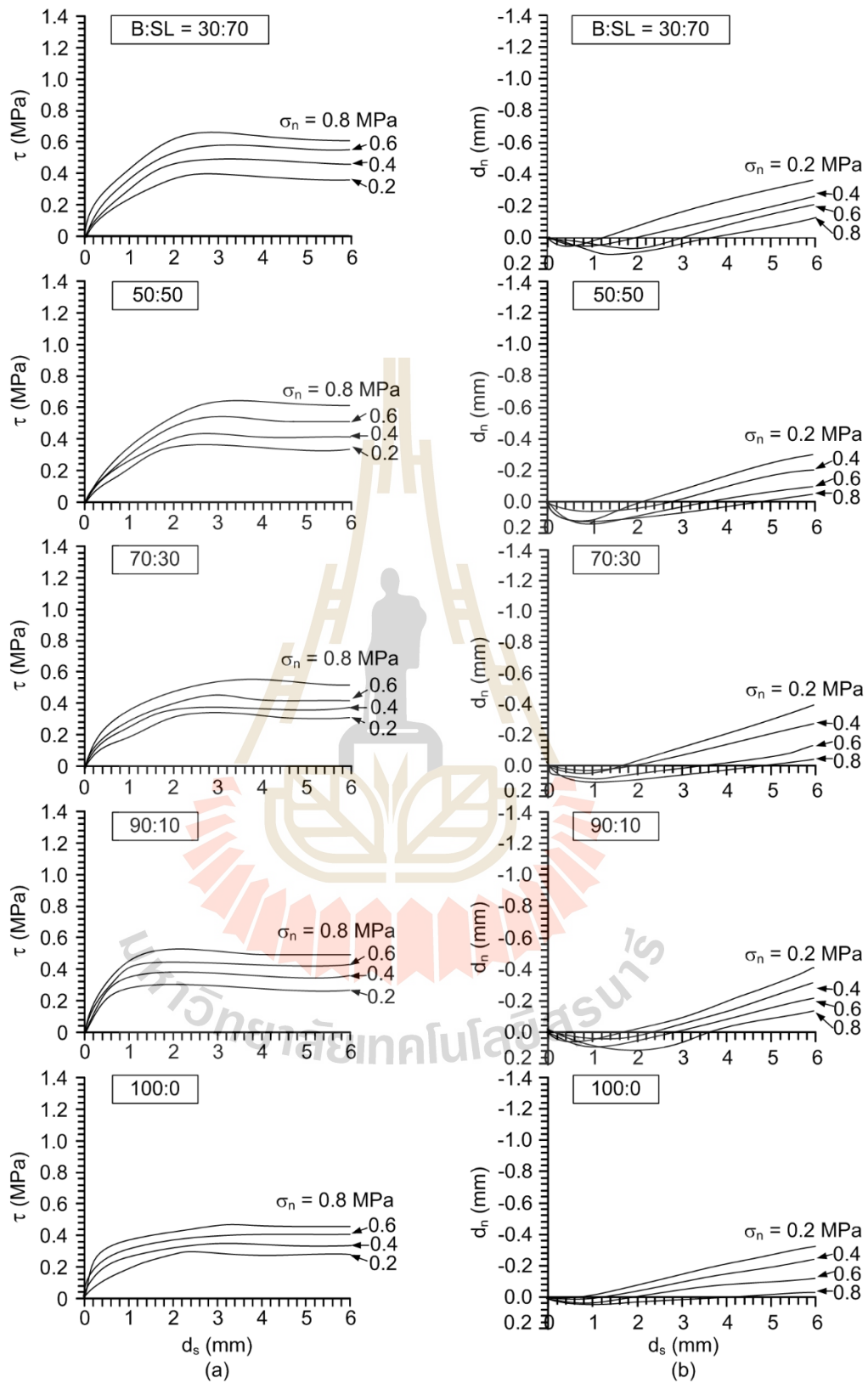


**Figure 4.5** Shear stress (a) and normal displacement (b) as a function of shear displacement for bentonite-sludge mixtures.

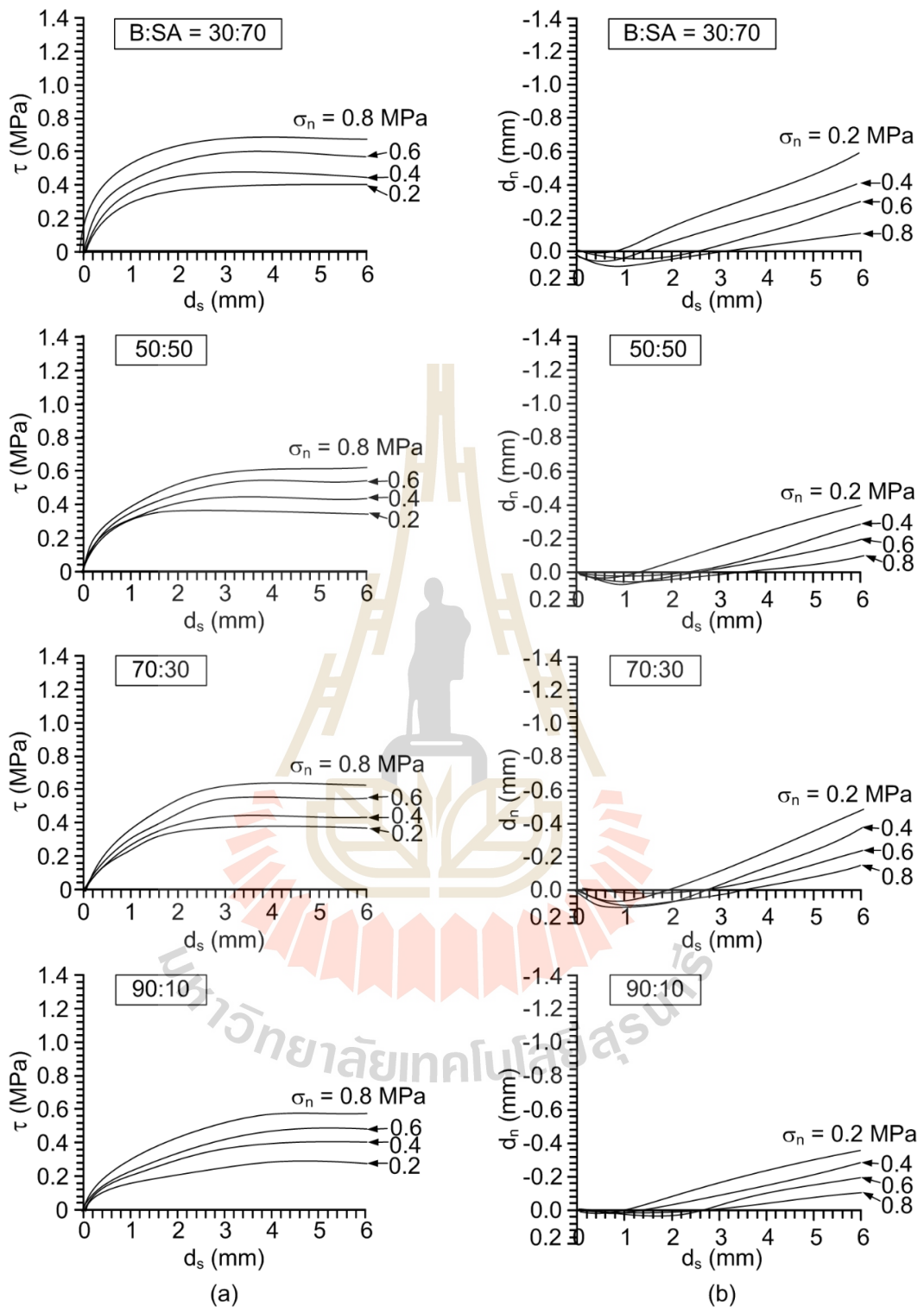


**Figure 4.6** Shear stress (a) and normal displacement (b) as a function of shear displacement for bentonite-sand mixtures.

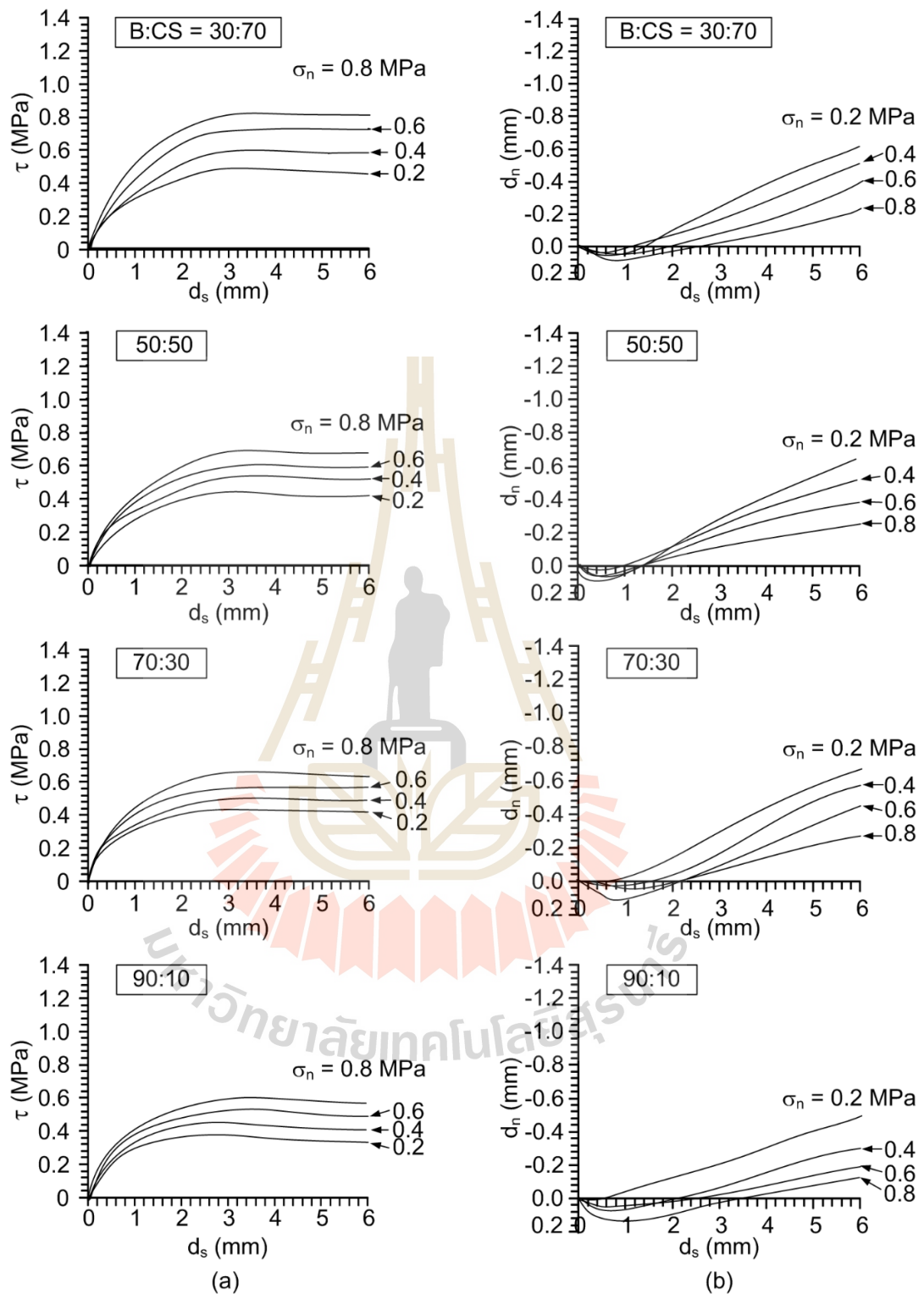


**Figure 4.7** Shear stress (a) and normal displacement (b) as a function of shear displacement for bentonite-crushed salt mixtures.

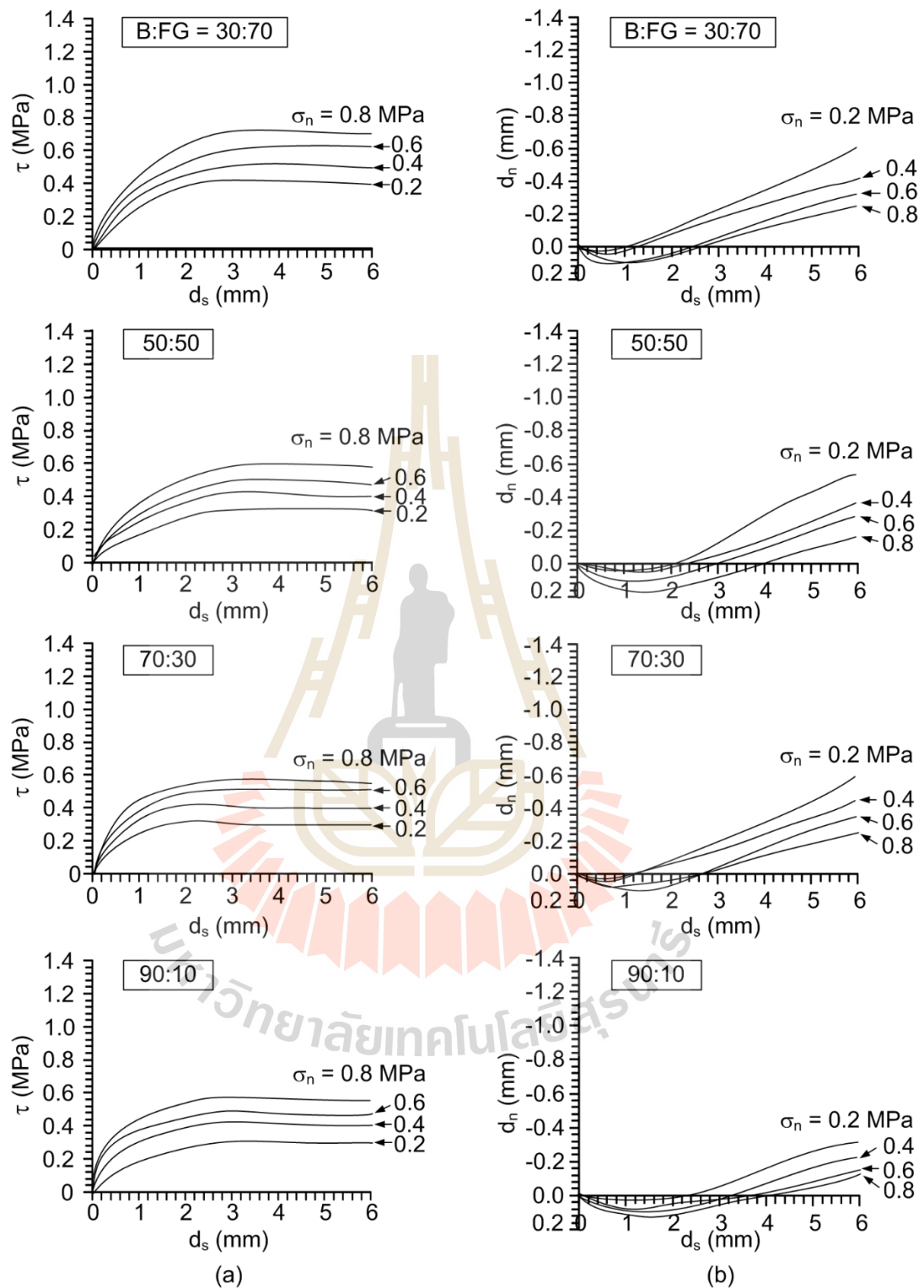


**Figure 4.8** Shear stress (a) and normal displacement (b) as a function of shear displacement for bentonite-fine gravel mixtures.

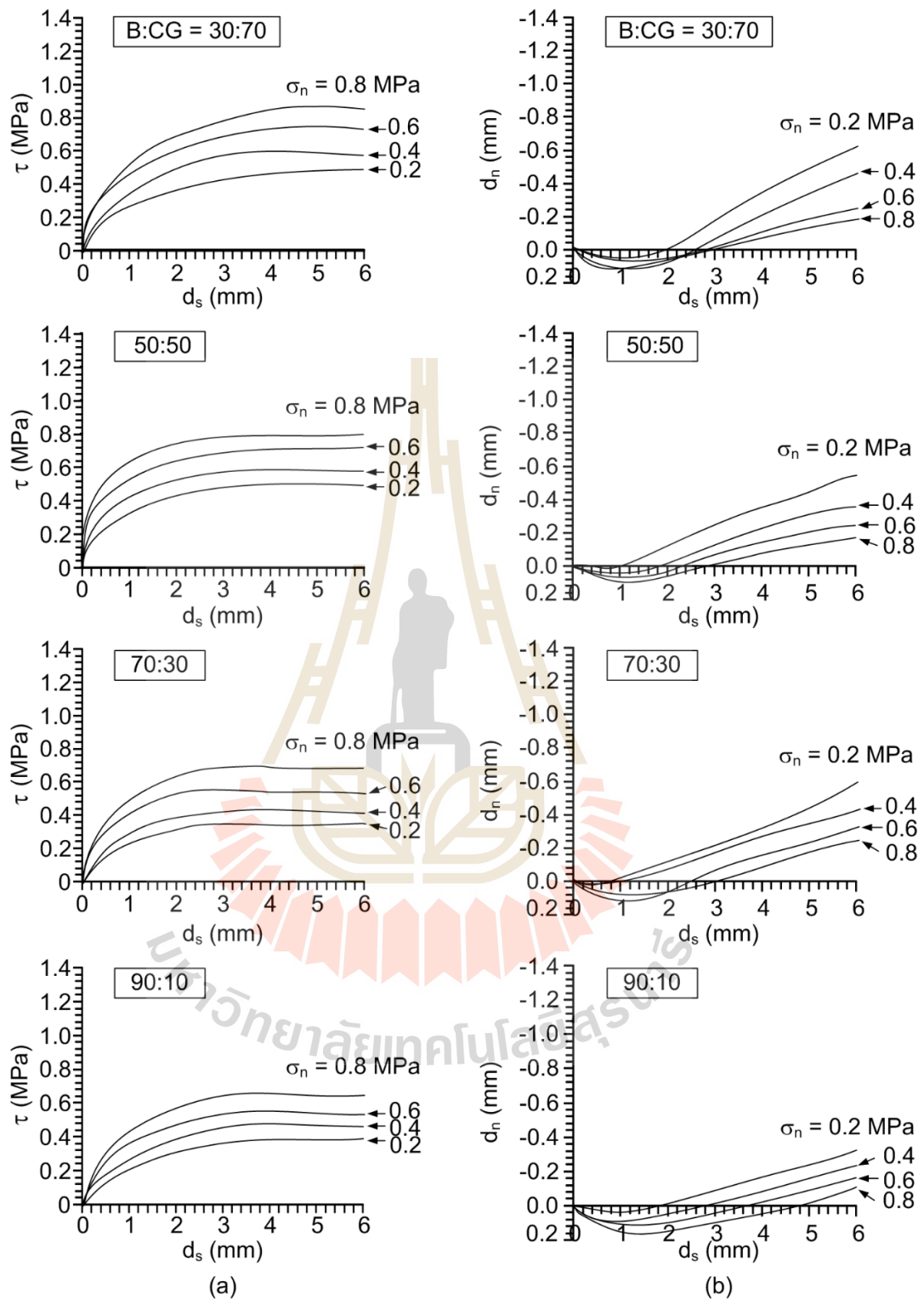


**Figure 4.9** Shear stress (a) and normal displacement (b) as a function of shear displacement for bentonite-coarse gravel mixtures.

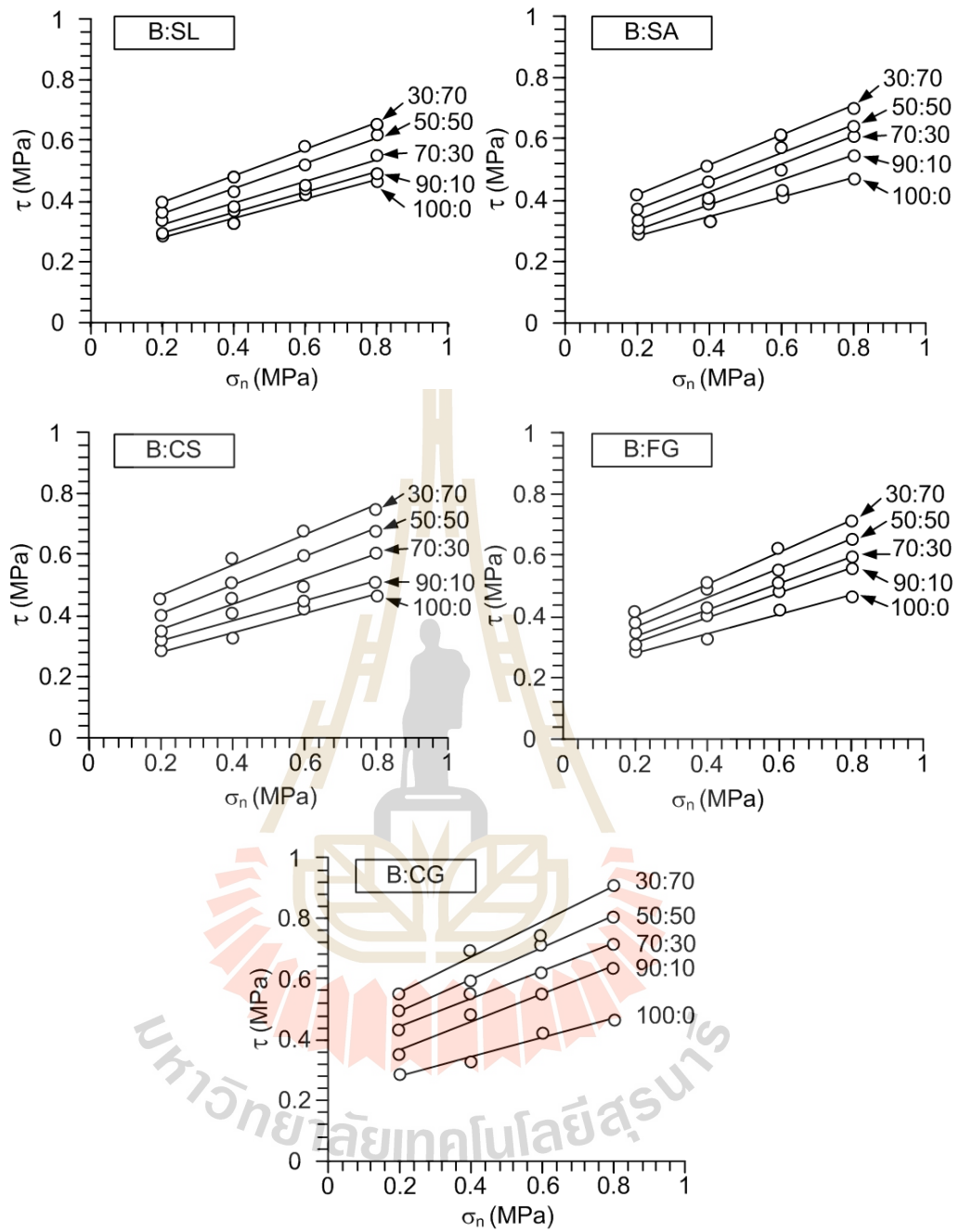


**Figure 4.10** Shear strengths as a function normal stress.

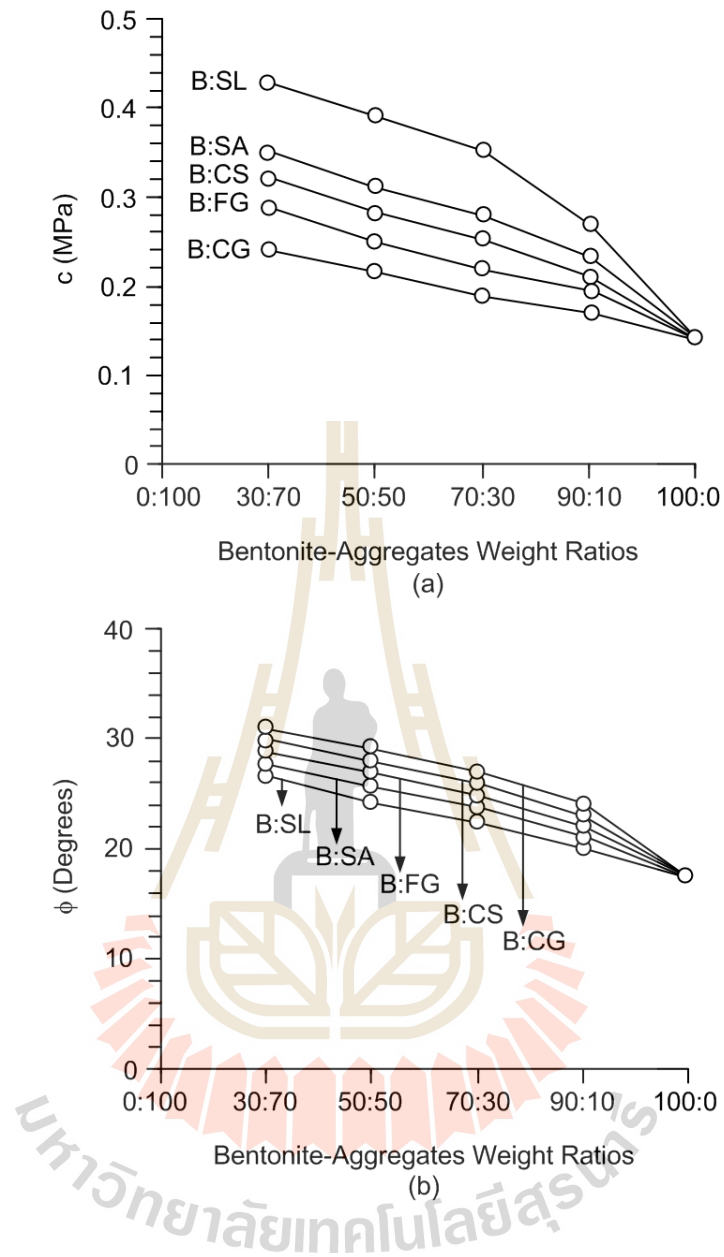


**Figure 4.11** Cohesions (a) and friction angles (b) as a function of bentonite-aggregates weight ratio.

**Table 4.2** Direct shear test results.

<b>Bentonite (B) : Aggregates</b>	<b>Weight ratio</b>	<b>c (MPa)</b>	<b>Friction angles (<math>\phi</math>)</b>	<b>R<sup>2</sup></b>
Bentonite : Sludge (B:SL)	100:0	0.14	18	0.974
	90:10	0.30	20	0.988
	70:30	0.36	23	0.956
	50:50	0.39	25	0.979
	30:70	0.43	27	0.990
Bentonite : Sand (B:SA)	90:10	0.25	22	0.931
	70:30	0.28	24	0.957
	50:50	0.32	26	0.995
	30:70	0.35	28	0.975
Bentonite : Crushed Salt (B:CS)	90:10	0.22	23	0.979
	70:30	0.28	26	0.949
	50:50	0.28	28	0.948
	30:70	0.33	29	0.996
Bentonite : Fine Gravel (B:FG)	90:10	0.20	24	0.942
	70:30	0.22	27	0.927
	50:50	0.25	29	0.993
	30:70	0.29	30	0.978
Bentonite : Coarse Gravel (B:CG)	90:10	0.17	25	0.990
	70:30	0.19	28	0.965
	50:50	0.22	30	0.991
	30:70	0.24	32	0.996

## 4.5 Uniaxial Compression Test

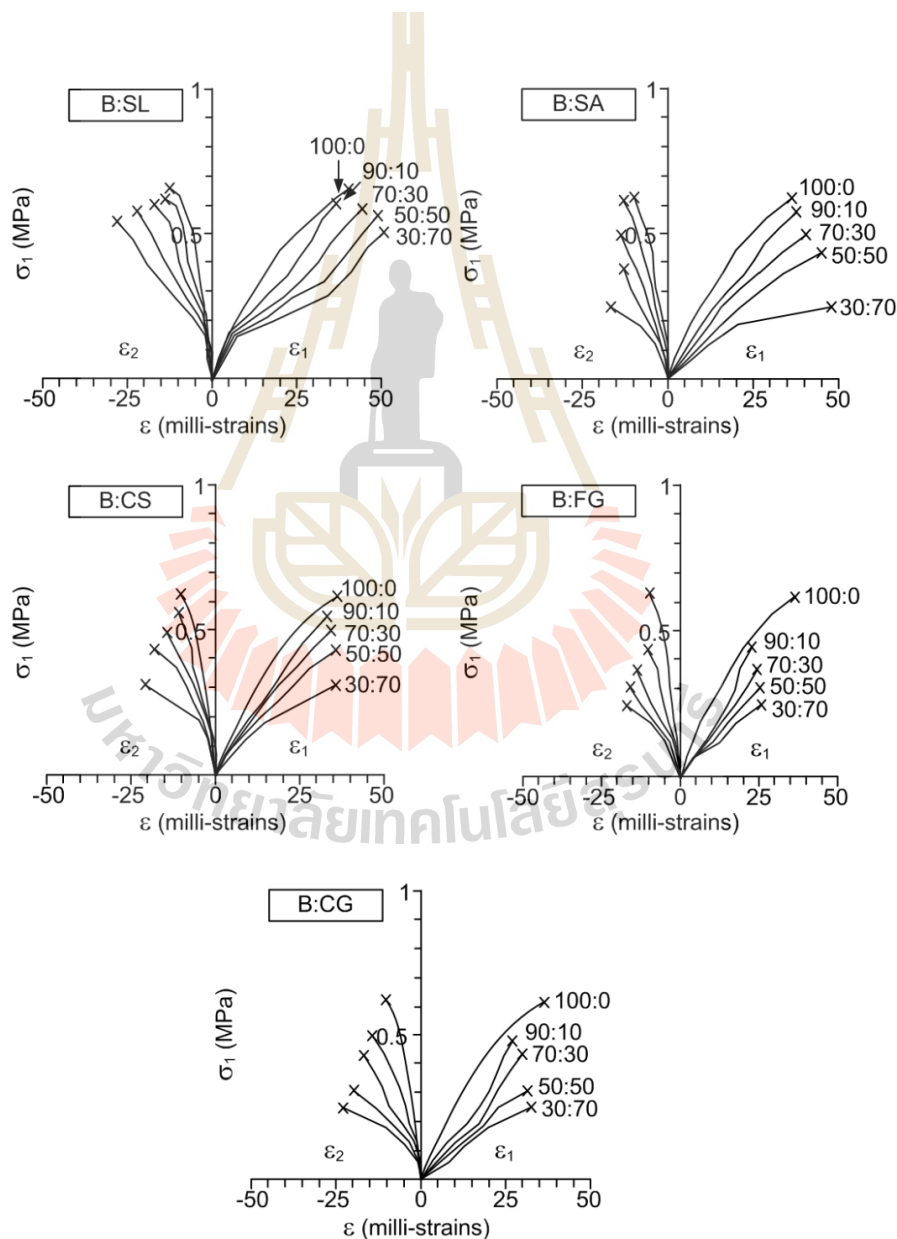
### 4.5.1 Test method

The compressive strength and elastic parameters of the compacted mixtures under their optimum brine content and maximum dry density can be determined by removing the specimen out of the three-ring mold. The specimen ends are cut to obtain flat and parallel surfaces. The length-to-diameter ratios are about 2.0-2.2. The compressive strengths are determined by axially loading under constant rate of 0.5-1 MPa/second until failure. Neoprene sheets are used to minimize the friction at the interfaces between the loading platen and the sample surface. The axial and lateral displacements are monitored. The compressive strength, Secant modulus ( $E_{sec}$ ) and Poisson's ratio are determined in accordance with the ASTM (D2938-95) standard practice.

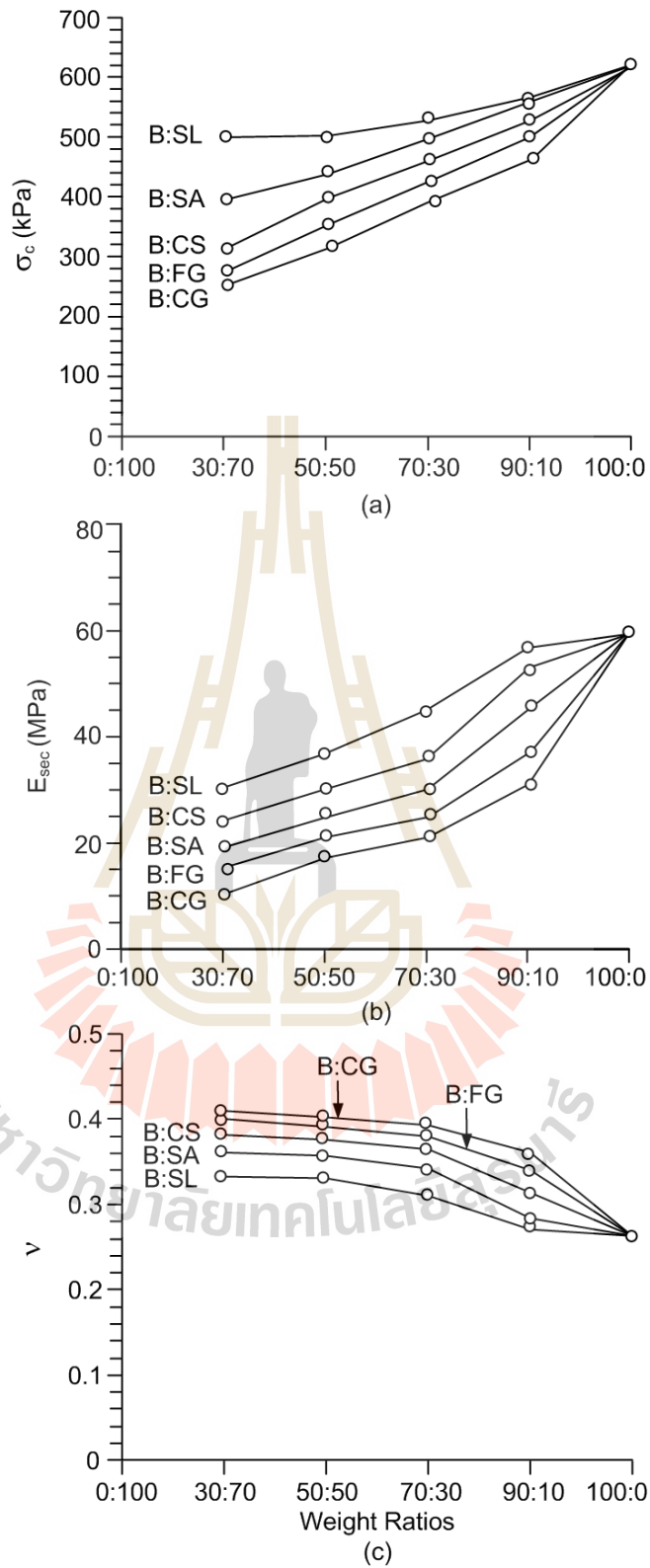
### 4.5.2 Uniaxial compression test results

Figure 4.12 shows the stress-strain curves obtained from different bentonite weight ratios and types of aggregate from start loading until failure. Figure 4.13 shows the compressive strength, elastic moduli and Poisson's ratios of all mixtures as a function of bentonite-aggregate weight ratio. The mixtures with higher bentonite contents give greater compressive strengths and elastic moduli than those with the lower one. The Poisson's ratio, however tends to decrease with the bentonite weight ratio. This is probably because the increase of bentonite content can densify the mixtures, and hence increases their strength and stiffness. The mixtures with finer aggregate particles (e.g. sludge and sand) tend to show higher strengths and elastic moduli than those with coarser aggregate particles (e.g. gravels). The Poisson's ratios of the coarser particles are greater than those of the finer ones. Because bentonite

effectively fills the smaller void spaces present between the individual fine particles in comparison to relatively larger void spaces between the coarse particles (Srikanth and Mishra, 2016). The porosity is a very important factor that affects the behavior of specimens, lower porosity leading to greater uniaxial compressive strength and Young's modulus. The test results are consistent with Ghazi (2015). They are summarized in Table 4.3.



**Figure 4.12** Stress-strain curves of uniaxial compression test.



**Figure 4.13** Compressive strengths (a), Secant moduli (b) and Poisson's ratio (c) as a function of bentonite-aggregates weight ratio.

**Table 4.3** Uniaxial compressive test results.

<b>Bentonite (B) : Aggregates</b>	<b>Weight ratio</b>	<b>Compressive strengths (kPa)</b>	<b>Elastic moduli (MPa)</b>	<b>Poisson's ratio</b>
B:SL	100:0	621	60	0.26
	90:10	562	57	0.27
	70:30	530	45	0.31
	50:50	499	37	0.33
	30:70	480	30	0.33
B:SA	90:10	560	53	0.28
	70:30	497	36	0.34
	50:50	434	30	0.36
	30:70	400	24	0.36
B:CS	90:10	530	45	0.31
	70:30	460	30	0.36
	50:50	400	25	0.38
	30:70	311	19	0.38
B:FG	90:10	500	37	0.34
	70:30	430	25	0.38
	50:50	350	21	0.39
	30:70	280	15	0.40
B:CG	90:10	460	31	0.36
	70:30	390	21	0.39
	50:50	310	17	0.40
	30:70	248	10	0.42

# CHAPTER V

## SWELLING TESTS

### 5.1 Introduction

Bentonite is most widely known for its ability to swell. It can absorb nearly 5 times its weight in water and at full saturation may occupy a volume 12 to 15 times its dry bulk (Odom, 1984). The high water absorption capacity of bentonite also makes it very plastic and resistant to fracturing or cracking. The behavior of the swelling capacity of compacted bentonite can be described in to three steps: before, during and after water absorption. Before water absorption, bentonite is composed of a mixture of montmorillonite, void, other nonswelling mineral and sand particle. During water absorption, montmorillonite absorbs water and into interlayers and swells occupying the void in the bentonite. Therefore, the volume of montmorillonite increases and the swelling capacity occurs. Finally, after water absorption, there is not any void to absorb, hence the volume of montmorillonite cannot further increase. At this point, the swelling capacity of compacted bentonite can be measured (Komine and Ogata, 1996). This chapter is to observe the free swelling behavior of sample with bentonite weight ratios, and the swelling of bentonite-aggregates under vertical stress changes. The mixtures with  $MgCl_2$  and  $NaCl$  brines are compared in this study.

## 5.2 Swelling Tests under Different Bentonite Weight Ratios

The weight ratios of bentonite-coarse gravel from 30:70, 50:50, 70:30 and 100:0 are studied. After compaction, the top surface is trimmed to obtain smooth surface. The sand (porous media) is placed on the top of the sample (Figure 5.1). The sample is submerged under brine. The swelling are recorded every 5 minutes by displacement dial gage. Swelling capacity is defined as (ASTM D4546-08 standard):

$$D = (\Delta H/H) \times 100 \quad (5.1)$$

where D is swelling ratio (%), H is the initial height and  $\Delta H$  is the change of the height.

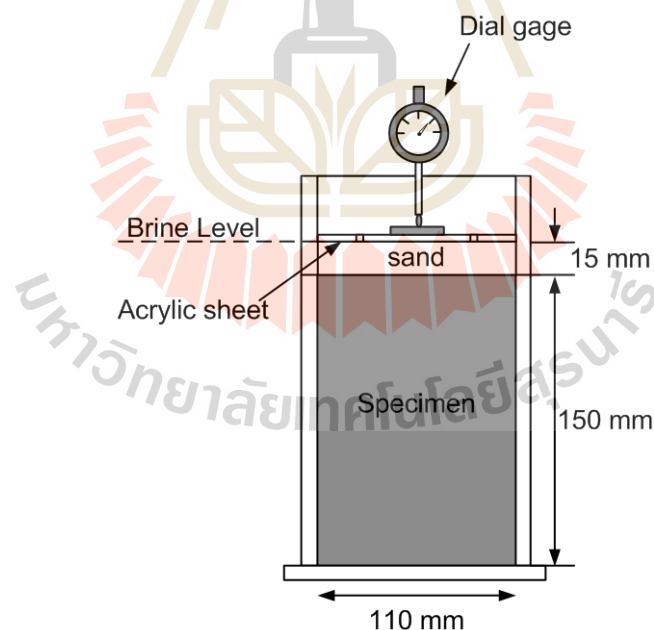


**Figure 5.1** Swelling test in three-ring compaction mold.

Swelling capacity by various bentonite weight ratios are presented in Figure 5.2. The results indicated that the maximum swelling capacity shows an exponential increase with increasing the bentonite weight ratio. Under both brines the swelling increases rapidly within the first days. It trends to remain constants for all weight ratio after 10 days under the brines. This is because Na-montmorillonite bentonite characteristically swells into water many times its dry volume. This agrees well with the results obtained by Gonzalez (2013). The mixtures with  $MgCl_2$  brine give higher swelling capacity than with NaCl brines. Suzuki et al. (2005) offer an explanation that it might be due to a decrease in double layer swelling between quasicrystals by NaCl. As the electronic double layer adjacent to the quasicrystal surface is compressed with increasing NaCl concentration, the aggregate swelling may decrease.

### **5.3 Swelling Tests under Different Aggregate Types**

The mixture of bentonite-to-aggregates of 30:70 are compacted using sludge, sand, crushed salt, fine and coarse gravels. This weight ratio is recommended by Butcher (1993), Borgesson et al. (2003) and Johannesson and Nilsson (2006). Less bentonite may become isolated in individual pores, reducing its effectiveness for wicking brine from other regions of the backfill; more bentonite will reduce the quasi-static rigidity provided by the granular skeleton within the mixture, and increase the cost of the backfill (Butcher, 1993). Using Eqs. (5.1) the swelling capacity can be calculated.

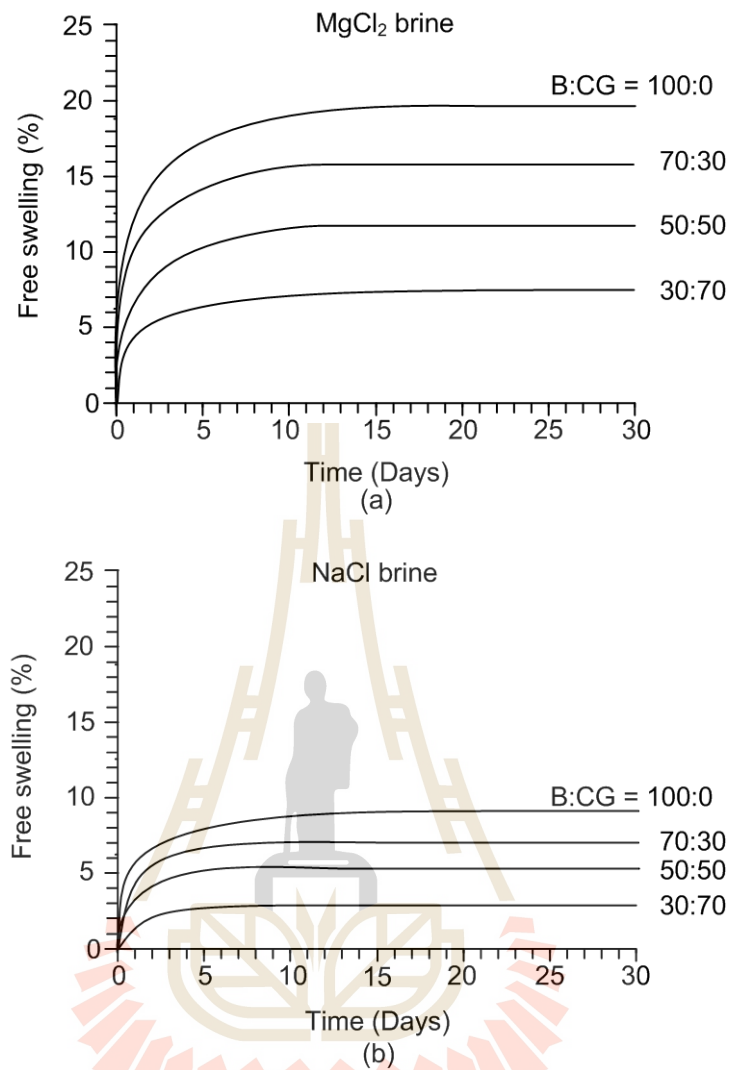


**Figure 5.2** Swelling capacity by various bentonite weight ratios for mixtures with MgCl<sub>2</sub> (a) and NaCl (b) brines.

From the data in Figure 5.3 the swelling capacity tends to decrease with increasing particle size. Fine particles (sludge) exhibits relatively higher swelling in comparison to coarse particles (coarse gravel). This may be because bentonite can effectively fill the smaller void spaces present between the individual fine particles in comparison to relatively larger void spaces between the coarse particles. Once the void spaces between fine particles are filled the bentonite will start to push the aggregates, resulting in a higher value of swelling capacity (Srikanth and Mishra, 2016).

#### **5.4 Swelling Tests under Different Vertical Stresses**

Four pure bentonite specimens have been used in the swelling under vertical stress tests. The vertical stresses of 0, 20, 50 and 100 kPa are used. The brine is always added on the specimen for 3 days following the ASTM (D4546-08) standard. The vertical swelling deformation is measured every 5 minutes.

Swelling results of compacted bentonite specimens under different vertical stresses are presented in Figure 5.4. Results show that the vertical stress is an important factor controlling the swelling capacity. The swelling capacity decreases with increasing vertical stress. The vertical stress may affect the internal structures of the compacted bentonite specimens, resulting in a reduction of the distance between aggregates and leading to the decrease of swelling strain. Under lower vertical stresses, the mixtures with  $MgCl_2$  brine give higher swelling capacity than those with  $NaCl$  brine. The difference becomes less under higher vertical stresses. Neiwphueng (2016) also observes that the bentonite with  $NaCl$  brine give lower swelling capacity than with  $MgCl_2$  brine. This also agrees well with the results obtained by Shariatmadari et al. (2011).

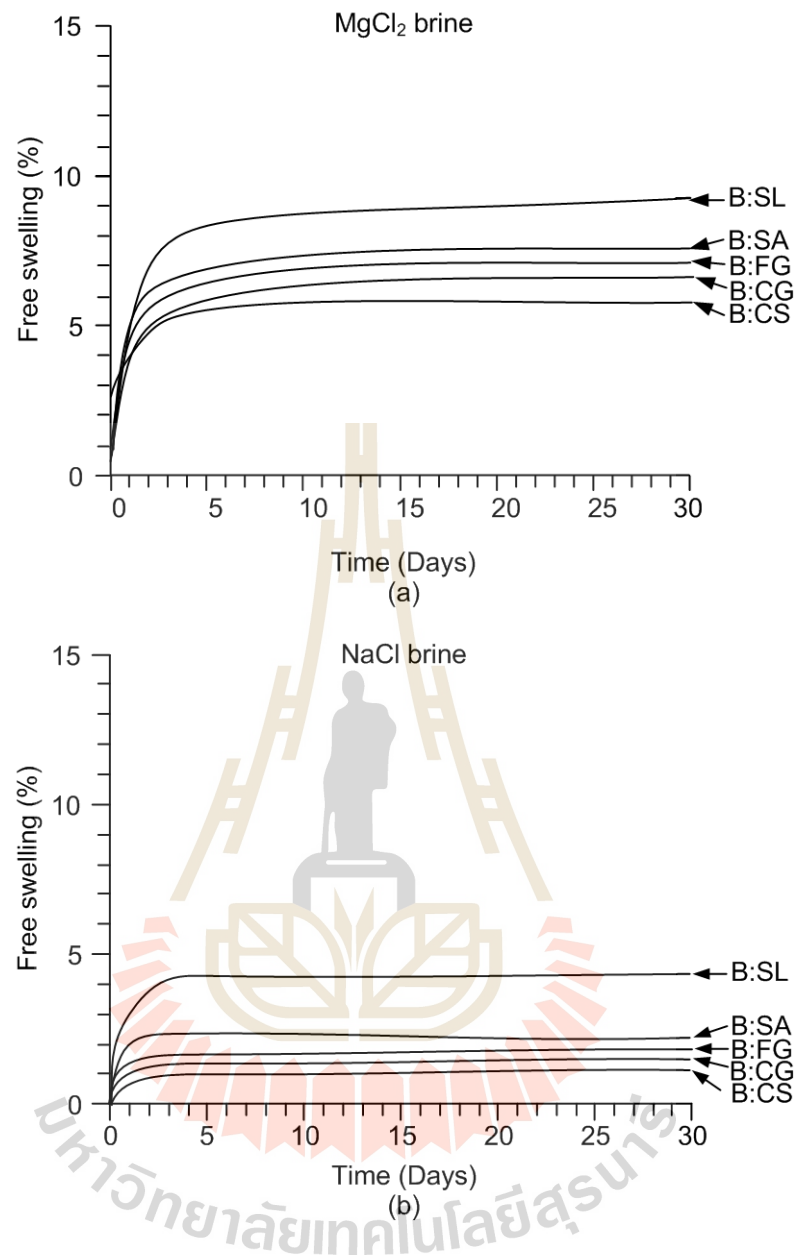


**Figure 5.3** Swelling capacity of different aggregate mixtures under MgCl<sub>2</sub> (a) and NaCl (b) brines.

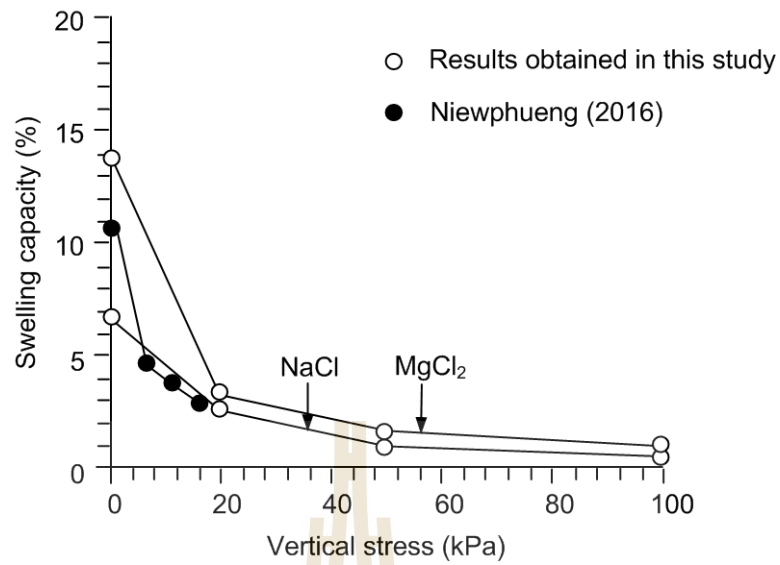


**Figure 5.4** Swelling capacity of pure bentonite as a function of vertical stresses, comparing between NaCl and MgCl<sub>2</sub> brine submersions.

## CHAPTER VI

### SCANNING ELECTRON MICROSCOPE ANALYSIS

#### 6.1 Introduction

This chapter describes the influence of  $MgCl_2$  and  $NaCl$  brines on the microstructures of compacted bentonite. The microstructures of compacted specimens under optimum brine contents are observed using scanning electron microscope (SEM). Each mixture is scanned before and after the swelling test, and hence the effect of swelling behavior can be revealed microscopically.

#### 6.2 Test Apparatus

Scanning electron microscope (SEM), JEOL JSM-6010LV, is a type of electron microscope that produces images of a sample by scanning the surface with a focused beam of electrons (Figure 6.1). The electrons interact with atoms in the controlled mixtures, producing various signals that contain information about the sample's surface topography. The electron beam is generally scanned in a raster scan pattern, and the beam's position is combined with the detected signal to produce an image. SEM can achieve resolution better than 1 nanometer.



**Figure 6.1** JEOL JSM-6010LV scanning electron microscope used in this studied.

### 6.3 Test Method

Pure bentonite specimens under optimum  $\text{MgCl}_2$  and  $\text{NaCl}$  brine content are observed in this study. All specimens are compacted to obtain maximum dry density and at optimum brine content. Two sets of specimens are prepared from each mixture. The first set is used to observe microstructure of the compacted bentonite mixtures. The second set is used to observe the swelling of bentonite under each brine. All specimens have been prepared to obtain nominal dimensions of  $1 \times 1 \times 1 \text{ cm}^3$  which are small enough to fit on the SEM specimen holder (Figure 6.2).

After the specimens are oven-dried at  $105 \pm 5^\circ \text{C}$  for 24 hours, they are coated with a gold film to become electrically conducting material. The specimens are prepared to withstand the vacuum conditions and the high energy beam of electrons.

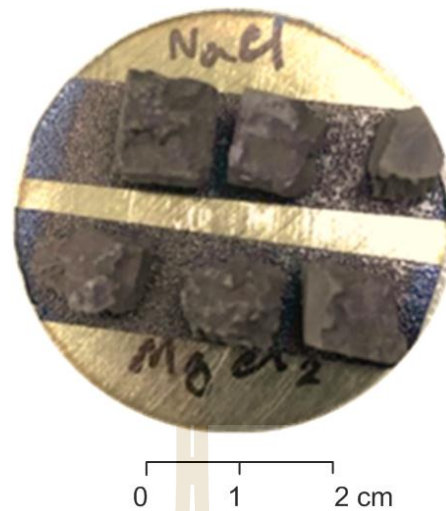


**Figure 6.2** Some specimens prepared for investigation under scanning electron microscope (SEM).

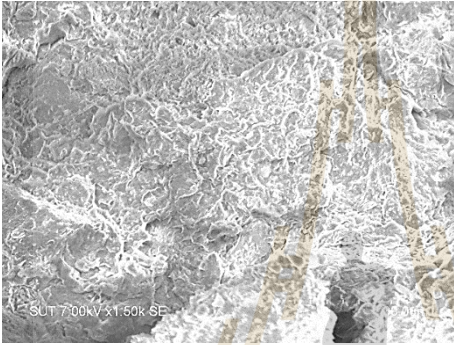
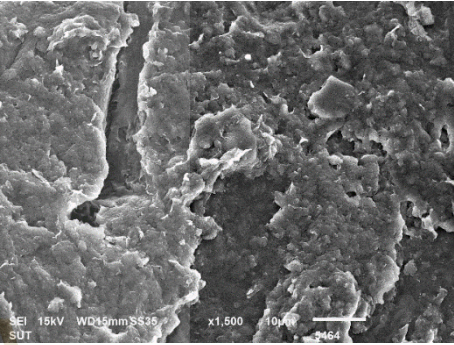
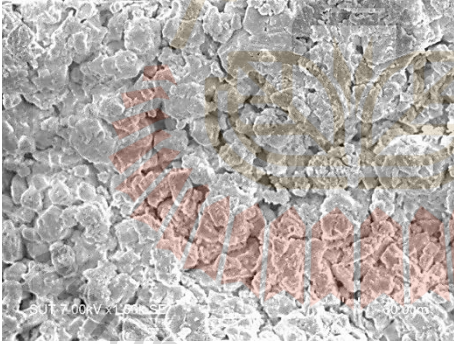
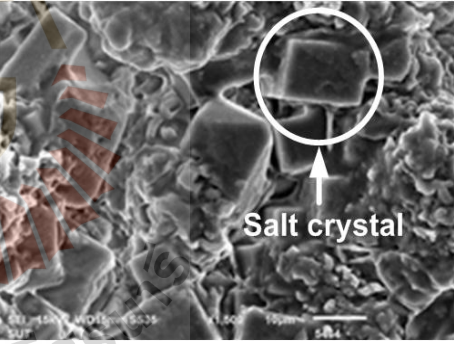
#### 6.4 Test Results

The SEM images of the compacted bentonite are shown in Table 6.1. Before different characters of the formed microstructures from different brines can be observed. The microstructure of the bentonite mixed with  $MgCl_2$  brine shows large amounts of leafs placed very closely to each other, and thus creating compact orientated layers of smectite particles. The bentonite mixed with  $NaCl$  brine shows more granular particles, which is characterized by large open-air voids.

After swelling, the layers of smectite particles swells and hence occupying voids in the bentonite. The SEM observations clearly show that the recrystallization mechanism does not occurred in the  $MgCl_2$  brine. On the other hand, the bentonite mixed with  $NaCl$  brine shows salt crystals that form in the specimen. The cubical shape (see in Table. 6.1) can be clearly seen. The differences of microstructures between mixtures mixed with  $MgCl_2$  and  $NaCl$  brines are also reflected in the forms of swelling

capacity. The mixture with  $\text{MgCl}_2$  brine gives higher swelling capacity than that with  $\text{NaCl}$  brine. This is probably because the  $\text{MgCl}_2$  brine cannot recrystallize as quickly as the  $\text{NaCl}$  brine (Suzuki et al., 2005).

**Table 6.1** SEM images of compacted bentonites with  $\text{MgCl}_2$  and  $\text{NaCl}$  brines.

Brines	Before swelling	After swelling
$\text{MgCl}_2$		
$\text{NaCl}$		

## CHAPTER VII

### DISCUSSIONS AND CONCLUSIONS

#### 7.1 Discussions

The objective of this study is to determine the mechanical performance of the compacted bentonite mixed with aggregates and saturated magnesium brine. The effort includes compaction, direct shear, uniaxial compressive strength and swelling tests on the mixtures for use as backfill materials in salt and potash mine openings. The aggregates are sludge, sand, crushed salt and fine and coarse gravels. Their grain sizes range from 0.425 to 10 mm. The mixing ratios of the bentonite-aggregate are from 30:70 to 100:0 by weight.

The compaction test results indicate that the maximum dry densities and the optimum  $\text{MgCl}_2$  brine contents depend largely on the particle sizes of the aggregate and the bentonite contents. The decrease of the bentonite weight ratio increases the dry density and decreases the optimum  $\text{MgCl}_2$  brine content. This agrees reasonably well with the test results obtained by Kaya and Durakan (2004) and Soltani-Jigheh and Jafari (2012). The mixtures which 30% bentonite and 70% aggregate exhibit relatively high maximum dry density. Similar trend for the maximum dry density and optimum  $\text{MgCl}_2$  brine content of 30:70 mixture was observed by Johannesson and Nilsson (2006) who conduct the compaction test on bentonite-crushed rock. The coarser particles show higher maximum dry density and lower optimum brine contents. This is supported by Srikanth and Mishra (2016).

Within the range of the normal stresses used here (0.2 to 0.8 MPa) the shear behavior of the mixtures relations can be well described by Coulomb criterion. The mixtures with coarser particles show higher friction angles and lower cohesions. These shear properties increase with increasing aggregate contents and angularity. The results also agree with those of Yanrong (2013) who studied the effects of particle shape and size distribution on the constitutive behavior of composite soils.

The compressive strengths and elastic moduli of the mixtures increase with increasing bentonite content. The mixtures containing finer particles show higher strength and stiffness than those containing coarser particles. This is because the fine particles effectively fill the small void spaces leading to greater compressive strength and Young's modulus. Similar behavior is observed by Srikanth and Mishra (2016).

Decreasing of the bentonite contents can decrease the swelling capacity of the mixtures. The bentonite can swell in water many times its dry volume (Odom, 1984). This agrees reasonably well with the test results obtained by Agus et al. (2010) and Cui et al. (2012). The swelling capacity decreases with increasing particles size of the aggregates and vertical stresses. This may be because bentonite can effectively fill the smaller void spaces present between the individual fine particles in comparison to relatively larger void spaces between the coarse particles.

SEM images show that microstructures of compacted bentonite do not show the recrystallization of the  $MgCl_2$  brine. On the other hand, the bentonite mixed with NaCl brine can show the salt crystals that formed on the sample and the structure shape which can be seen under microscope. The results clearly show that the mixtures with NaCl brine give lower swelling capacity than those with  $MgCl_2$  brine. This is due to a decrease in double layer swelling between quasicrystals by NaCl (Suzuki et al., 2005).

## 7.2 Conclusions

1. Decrease of the bentonite contents gives higher dry densities and shear strength of the mixtures. This is due to the fact that the aggregate densities are greater than that of the bentonite. Low bentonite contents show lower compressive strength because bentonite do not densify the mixtures.

2. Coarser particles give higher dry densities than those with finer particles. This is because the coarser particles have higher density than the finer particles. The mixtures with coarser particles show higher friction angles and lower cohesions. The cohesions and friction angles also increase with increasing angularity of the aggregates. The compressive strengths and elastic moduli of the mixtures containing finer particles are higher than those mixed with coarser particles.

3. The swelling behavior depending on bentonite contents, its ability to swell. The swelling capacity decreases with decreasing bentonite contents and particles size of the aggregates.

4. Mixture of 30% bentonite and 70% aggregate may be suitable because it shows highest maximum dry densities, shear strengths, and can decrease the cost of the backfill materials. As suggested by Butcher (1993), Borgesson, et al. (2003) and Johannesson and Nilsson (2006) that for effective compaction the bentonite weight ratio for the mixtures should not be less than 30%. This is primarily to prevent bridging and voids occurring between aggregates particles.

5. The carnallite and halite (rock salt) are insensitive to  $MgCl_2$  brine as suggested by Theerapun et al. (2017). The magnesium brine is recommended for mixing with backfilling material the salt and potash mine openings. Selection of the types and contents of aggregates also depends on site-specific conditions and

availability of the materials. Bentonite, even construction-grade type, generally costs more than the aggregates. Crusted salt and sludge are considered as waste products and are relatively inexpensive as compared to sand and gravel.

### **7.3 Recommendations for Future Studies**

The test results for the bentonite-aggregate mixture have been limited by testing time and diversity of aggregate types. To confirm the conclusions drawn in this study, more testing is required as follows:

1. The effects of consolidation stresses and period should be investigated and established the relation with the physical and mechanical properties of mixtures for long-term performance assessment.
2. Permeability should be used to obtain mixtures with different the bentonite weight ratio and aggregates.
3. More testing is required on a variety of aggregate types and particle sizes.

## REFERENCES

- Agus, S.S., Schanz, T., and Fredlund, D.G. (2010). Measurements of suction versus water content for bentonite-sand mixtures. **Canadian Geotechnical Journal**. 47(5): 583-594.
- ASTM D1557-12. (2012). **Standard Test Methods for Laboratory Compaction Characteristics of Soil Using Modified Effort (56,000 ft-lbf/ft<sup>3</sup> (2,700 kN-m/m<sup>3</sup>))**. In Annual Book of ASTM Standards. Philadelphia: American Society for Testing and Materials.
- ASTM D2938-95. (1995). **Standard Test Method for Unconfined Compressive Strength of Intact Rock Core Specimens**. In Annual Book of ASTM Standards. Philadelphia: American Society for Testing and Materials.
- ASTM D3080-11. (2011). **Standard Test Method for Direct Shear Test of Soils Under Consolidated Drained Conditions**. In Annual Book of ASTM Standards. Philadelphia: American Society for Testing and Materials.
- ASTM D4546-08. (2008). **Standard Test Methods for One-Dimensional Swell or Collapse of Cohesive Soils**. In Annual Book of ASTM Standards. Philadelphia: American Society for Testing and Materials.
- Bagherzadeh-Khalkhali, A. and Mirghasemi, A.A. (2009). Numerical and experimental direct shear tests for coarse-grained soils. **Particuology**. 7(1): 83-91.

- Borgesson, L., Johannesson, L.E., and Gunnarsson, D. (2003). Influence of soil structure heterogeneities on the behavior of backfill materials based on mixtures of bentonite and crushed rock. **Applied Clay Science**. 23(1-4): 121-131.
- Butcher, B.M. (1993). **The Advantages of A Salt/Bentonite Backfill For Waste Isolation Pilot Plant Disposal Rooms**. Sandia Report, prepared from Sandia National Laboratories, Albuquerque, New Mexico.
- Chalermyanont, T. and Arrykul, S. (2005). Compacted sand-bentonite mixtures for hydraulic containment liners. **Songklanakarin Journal of Science and Technology**. 27(2): 313-323.
- Chen, Y.G., Zhu, C.M., Ye, W.M., Cui, Y.J., and Chen, B. (2016). Effect of solution concentration and vertical stress on the swelling behavior of compacted GMZ01 bentonite. **Applied Clay Science**. 124-125: 11-20.
- Cho, W.J., Kim, J.S., and Choi, J.W. (2011). Influence of water salinity on the hydraulic conductivity of compacted bentonite. **Journal of the Korean Radioactive Waste Society**. 9(4): 199-206.
- Chun-Ming, Z., Wei-Min, Y., Yong-Gui, C., Bao, C., and Yu-Jun, C. (2013). Influence of salt solutions on the swelling pressure and hydraulic conductivity of compacted GMZ01 bentonite. **Engineering Geology**. 166: 74-80.
- Cui, S.L., Zhang, H.Y., and Zhang, M. (2012). Swelling characteristics of compacted GMZ bentonite-sand mixtures as a buffer/backfill material in china. **Engineering Geology**. 141-142(3): 65-73.
- Di Maio, C. and Scaringi, G. (2016). Shear displacements induced by decrease in pore solution concentration on a pre-existing slip surface. **Engineering Geology**. 200: 1-9.

- Dixon, D.A., Gray, M.N., and Thomas, A.W. (1985). A study of the compaction properties of potential clay-sand buffer mixtures for use in nuclear fuel waste disposal. **Engineering Geology**. 21(3-4): 247-255.
- Frankovská, J., Andrejkovičová, S., and Janotka, I. (2010). Effect of NaCl on hydraulic properties of bentonite and bentonite-palygorskite mixture. **Geosynthetics International**. 17(4): 250-259.
- Fuenkajorn, K. and Daemen, J. J. K. (1988). **Borehole Closure in Salt**. Technical Report, prepared from the U.S. Nuclear Regulatory Commission, Washington, D.C. by the University of Arizona.
- Fuenkajorn, K. and Daemen, J.J.K. (Eds.), 1996. **Sealing of Boreholes and Underground Excavations in Rock**. Chapman and Hall, London.
- Ghazi, A. F. (2015). Engineering Characteristics of Compacted Sand-Bentonite Mixtures. **Master Thesis**, Edith Cowan University.
- González, S.S. (2013). The Swelling Pressure of Bentonite and Sand Mixtures. **Master Thesis**, KTH Royal Institute of Technology.
- Holtz, R. D., Kovacs, W. D., and Sheahan, T. C. (1981). **An Introduction to Geotechnical Engineering** (Vol. 733). Englewood Cliffs, NJ: Prentice-Hall.
- Johannesson, L.E. and Nilsson, U. (2006). **Geotechnical Properties of Candidate Backfill Material for Deep Repository**, Technical Report, Svensk Kärnbränslehantering AB.
- Kaya, A. and Durukan, S. (2004). Utilization of bentonite-embedded zeolite as clay liner. **Applied Clay Science**. 25(1-2): 83-91.

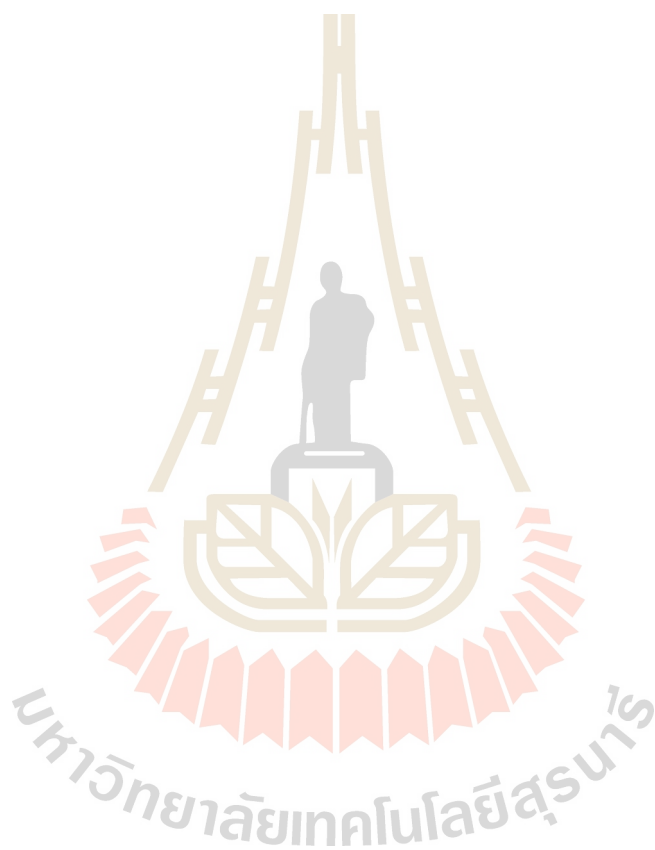
- Khamrat, S., Tepnarong, P., Artkhonghan, K., and Fuenkajorn, K. (2018). Crushed salt consolidation for borehole sealing in potash mines. **Geotechnical and Geological Engineering**. 36(1): 49-62.
- Kim, D. and Ha, S. (2014). Effects of particle size on the shear behavior of coarse grained soils reinforced with geogrid. **Materials**. 7(2): 963-979.
- Komine, H. and Ogata, N. (1996). Prediction for swelling characteristics of compacted bentonite. **Canadian Geotechnical Journal**. 33: 11-22.
- Lim, S.C., Gomes, C., and Kadir, M.Z.A.A. (2013). Characterizing of Bentonite with Chemical, Physical and Electrical Perspectives for Improvement of Electrical Grounding Systems. **International Journal of Electrochemical Science**. 8: 11429-11447.
- Madsen, F.T. and Müller-Vonmoos, M. (1989). The swelling behaviour of clays. **Applied Clay Science**. 4(2):143-156.
- Mašín, D. and Khalili, N. (2015). Swelling phenomena and effective stress in compacted expansive clays. **Canadian Geotechnical Journal**. 53(1): 134-147.
- Navarro, V., Yustres, Á., Asensio, L., De la Morena, G., González-Arteaga, J., Laurila, T., and Pintado, X. (2017). Modelling of compacted bentonite swelling accounting for salinity effects. **Engineering Geology**. 223: 48-58.
- Neiwphueng, U. and Fuenkajorn, K. (2015). Compacted bentonite-crushed salt mixtures as sealants in rock salt and potash openings. In **Proceedings of the Ninth South East Asean Technical University Consortium Symposium** (pp. 326-329). Thailand.
- Niewphueng, U. (2016). Compacted Bentonite-Crushed Salt Mixtures as Sealants in Mine Openings. **Master Thesis**, Suranaree University of Technology.

- Odom, I. E. (1984). **Smectite Clay Minerals: Properties and Uses**. Philosophical Transactions of the Royal Society of London. Series A, Mathematical and Physical Sciences, 311(1517), pp. 391-409.
- Ouyang, S. and Daemen, J.J. (1992). **Sealing Performance of Bentonite and Bentonite/Crushed Rock Borehole Plugs**. Technical Report, prepared for the U.S Nuclear Regulatory Commission, Washington, DC by the University of Arizona.
- Pongpeng, K., Tepnarong, P., Artkhonghan, K., and Fuenkajorn, K. (2017). Performance assessment of three-ring compaction and direct shear mold for testing granular and clayey mixtures. In **Proceedings of the Eleventh South East Asean Technical University Consortium Symposium**. Viet Nam.
- Power, M.C. (1982). **Comparison Charts for Estimating Roughness and Sphericity**. AGI Data Sheets, American Geological Institute, Alexandria, VA.
- Proctor, R. (1933). **Fundamental Principles of Soil Compaction**. Engineering News-Record. 111(13).
- Proia, R., Croce, P., and Modoni, G. (2016). Experimental investigation of compacted sand-bentonite mixtures. **Procedia Engineering**. 158: 51-56.
- Ran, C. and Daemen, J.J.K. (1995). The influence of crushed salt particle gradation on compaction. In **Proceedings of The Thirty-fifth U.S. Symposium on Rock Mechanics** (pp.761-766). Reno. NV. A.A. Balkema, Rotterdam.
- Sattra, P. and Fuenkajorn, K. (2015). Shear strength of compacted sludge-crushed salt mixtures. In **Proceedings of the Ninth South East Asean Technical University Consortium Symposium** (pp. 322-325). Thailand.

- Savage, D. (2005). **The Effects of High Salinity Groundwater on The Performance Of Clay Barriers**. SKI Report, Swedish Nuclear Power Inspectorate (SKI).
- Shariatmadari, N., Salami, M., and Karimpour Fard, M. (2011). Effect of inorganic salt solutions on some geotechnical properties of soil-bentonite mixtures as barriers. **International Journal of Civil Engineering**. 9(2): 103-110.
- Soltani-Jigheh, H. and Jafari, K. (2012). Volume change and shear behavior of compacted clay-sand/gravel mixtures. **International Journal of Engineering and Applied Sciences**. 4: 52-66.
- Sonsakul, P. and Fuenkajorn, K. (2013). Development of three-ring compaction and direct shear test mold for soil with oversized particles. **Research and Development Journal of the Engineering Institute of Thailand under H.M. the King's Patronage**. 24(2): 1-7.
- Sonsakul, P., Walsri, C., Horvibolsuk, S., and Fuenkajorn, K. (2013). Shear strength and permeability of compacted bentonite-crushed salt seal. In **Proceedings of the Fourth Thailand Symposium on Rock Mechanics**. Thailand.
- Srikanth, V. and Mishra, A. K. (2016). A laboratory study on the geotechnical characteristics of sand-bentonite mixtures and the role of particle size of sand. **International Journal of Geosynthetics and Ground Engineering**. 2 (3): 1-10.
- Studds, P. G., Stewart, D. I., and Cousens, T. W. (1998). The effects of salt solutions on the properties of bentonite-sand mixtures. **Clay Minerals**. 33(4): 651-660.
- Suwanabut, W., Khamrat, S., and Fuenkajorn, K. (2017). Consolidation of crushed salt mixed with saturated  $MgCl_2$  brine. In **Proceedings of the Twelfth South East Asean Technical University Consortium Symposium**. Indonesia.

- Suzuki, S., Prayongphan, S., Ichikawa, Y., and Chae, B. (2005). In situ observations of the swelling of bentonite aggregates in NaCl solution. **Applied Clay Science**. 29, 89–98.
- Theerapun, C., Khamrat, S., Sartkeaw, S., and Fuenkajorn, K. (2017). Effects of backfill compositions on integrity of underground salt and potash mines. **Research and Development Journal of the Engineering Institute of Thailand under H.M. the King's Patronage**. 28(2): 15-22.
- Vangla, P. and Latha, G.M. (2015). Influence of particle size on the friction and interfacial shear strength of sands of similar morphology. **International Journal of Geosynthetics and Ground Engineering**. 1(6): 1-12.
- Villar, M.V. (2002). **Thermo-Hydro-Mechanical Characterization of A Bentonite From Cabo De Gata. A Study Applied to The Use of Bentonite as Sealing Material In High Level Radioactive Waste Repositories**. Publicación Técnica ENRESA 01/2002, Madrid.
- Wang, Q., Cui, Y.J., Tang, A.M., Delage, P., Gatmiri, B., and Ye, W.M. (2014). Long-term effect of water chemistry on the swelling pressure of a bentonite-based material. **Applied Clay Science**. 87: 157-162.
- Yanrong, L. (2013). Effects of particle shape and size distribution on the shear strength behavior of composite soils. **Bulletin of Engineering Geology and the Environment**. 72(3-4): 371-381.
- Zhang, L., Sun, D. A., and Jia, D. (2016). Shear strength of GMZ07 bentonite and its mixture with sand saturated with saline solution. **Applied Clay Science**. 132: 24-32.

Zhang, M., Zhang, H., Jia, L., and Cui, S. (2012). Salt content impact on the unsaturated property of bentonite–sand buffer backfilling materials. **Nuclear Engineering and Design**. 250: 35-41.



## **BIOGRAPHY**

Miss Laksikar Sitthimongkol was born on September 6, 1995 in Chiang Rai Province, Thailand. She received her Bachelor's Degree in Engineering (Geotechnology) from Suranaree University of Technology in 2017. For her post-graduate, she continued to study with a Master's degree in the Geological Engineering Program, Institute of Engineering, Suranaree university of Technology. During graduation, 2017-2019, she was a part time worker in position of research assistant at the Geomechanics Research Unit, Institute of Engineering, Suranaree University of Technology.

